ทองขนาดนาโนรองรับบนซิลิกาที่มีหมู่อะมิโด-อะมิดอกซีมสำหรับการดูดซับและ
ออกซิเดชันเชิงเร่งปฏิกิริยาของโทลูอีน

นางสาวปิยธิดา แสงห้วยไผ่
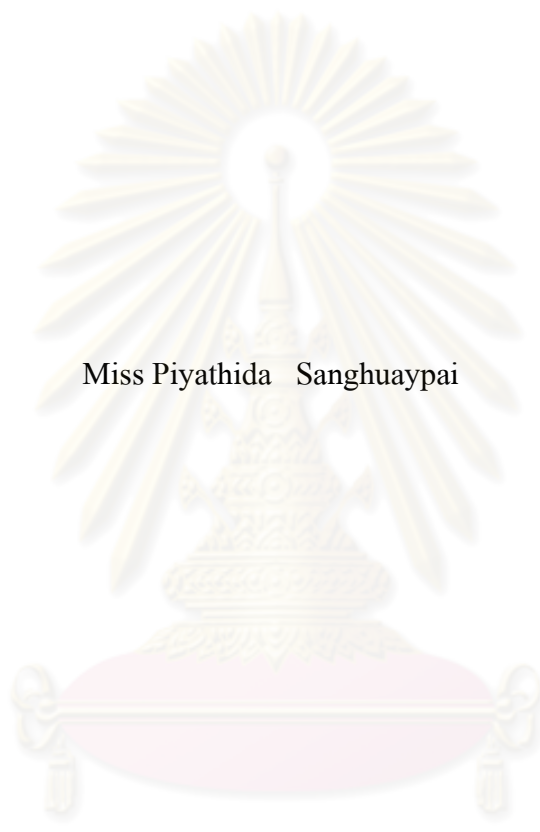
NANOGOLD SUPPORTED ON AMIDO-AMIDOXIME FUNCTIONALIZED SILICA

FOR ADSORPTION AND CATALYTIC OXIDATION OF TOLUENE

Miss Piyathida   Sanghuaypai

A Thesis Submitted in Partial Fulfillment of the Requirements

for the Degree of Master of Science Program in Petrochemistry and Polymer Science

Faculty of Science

Chulalongkorn University

Academic Year 2009

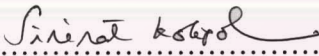| Thesis Title	NANOGOLD SUPPORTED ON AMIDO-AMIDOXIME FUNCTIONALIZED SILICA FOR ADSORPTION AND CATALYTIC OXIDATION OF TOLUENE
By	Miss Piyathida Sanghuaypai
Field of Study	Petrochemistry and Polymer Science
Thesis Advisor	Assistant Professor Apichat Imyim, Ph.D.
Thesis Co-Advisor	Assistant Professor Soamwadee Chaianansutcharit, Ph.D.

Accepted by the Faculty of Science, Chulalongkorn University in Partial Fulfillment of the Requirements for the Master's Degree
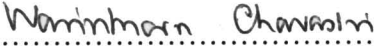
.... Dean of the Faculty of Science

(Professor Supot Hannongbua, Dr.rer.nat.)

THESIS COMMITTEE

....Chairman

(Associate Professor Sirirat Kokpol, Ph.D.)

....Thesis Advisor

(Assistant Professor Apichat Imyim, Ph.D.)

....Thesis Co-Advisor

(Assistant Professor Soamwadee Chaianansutcharit, Ph.D.)

.... Examiner

(Assistant Professor Warinthorn Chavasiri, Ph.D.)

.... External Examiner

(Anawat Pinisakul, Ph.D.)

ปิยธิดา แสงห้วยไผ่ : ทองขนาดนาโนรองรับบนซิลิกาที่มีหมู่อะมิโด-อะมิดอกซีมสำหรับ
การดูดซับและออกซิเดชันเชิงเร่งปฏิกิริยาของโทลูอีน. (NANOGOLD SUPPORTED ON
AMIDO-AMIDOXIME FUNCTIONALIZED SILICA FOR ADSORPTION AND
CATALYTIC OXIDATION OF TOLUENE) อ.ที่ปรึกษาวิทยานิพนธ์หลัก: ผศ.ดร.อภิชาติ
อิ่มยิ้ม, อ.ที่ปรึกษาวิทยานิพนธ์ร่วม: ผศ.ดร. โสมวดี ไชยอันต์สุจริต, 77 หน้า.

เตรียมทองขนาดนาโนรองรับบนซิลิกาที่มีหมู่อะมิโด-อะมิดอกซีม โดยการผสมซิลิกาเจลที่
มีหมู่ฟังก์ชันอะมิโด-อะมิดอกซีมในสารละลาย $HAuCl_4$ ตรวจหาลักษณะเฉพาะของทองขนาดนาโน
รองรับบนซิลิกาที่มีหมู่อะมิโด-อะมิดอกซีมด้วยเทคนิคการเลี้ยวเบนของรังสีเอกซ์, เทคนิคการ
ตรวจวัดพื้นที่ผิวและความมีรูพรุน ศึกษาการดูดซับไอระเหยของโทลูอีนบนอนุภาคนาโนของทอง
ตรวจวัดความจุของการดูดซับด้วยระบบฟิกซ์เบดที่อุณหภูมิห้องโดยใช้อาร์กอนเป็นแก๊สพา ศึกษา
ปัจจัยที่มีผลต่อประสิทธิภาพการดูดซับ ได้แก่ เวลาในการดูดซับ, อัตราการไหลของแก๊สพา และ
ปริมาณตัวดูดซับ ความจุการดูดซับเพิ่มขึ้นเมื่อเวลาในการดูดซับมากขึ้น และความจุการดูดซับลดลง
เมื่อเพิ่มอัตราการไหลของแก๊สพาและปริมาณตัวดูดซับ ความจุการดูดซับไอระเหยของโทลูอีนสูงสุด
มีค่าเท่ากับ 1.36 กรัมต่อกรัม ที่เวลา 45 นาที อัตราการไหลแก๊สพา 40 มิลลิลิตรต่อนาที และปริมาณ
ตัวดูดซับ 0.05 กรัม ศึกษาอิทธิพลของอุณหภูมิและความเข้มข้นของโทลูอีนในอากาศที่มีต่อการเกิด
ออกซิเดชันของไอของโทลูอีน โดยแบ่งการศึกษาเป็น 2 ระบบ ได้แก่ 1) ระบบต่อเนื่อง อุณหภูมิ และ
ความเข้มข้นของโทลูอีนที่ทำการศึกษาอยู่ในช่วง 25 – 175 องศาเซลเซียส และ 190 – 685 มิลลิกรัม
ต่อลูกบาศก์เมตร ตามลำดับ พบว่าค่าร้อยละการกำจัดโทลูอีนสูงสุดเท่ากับ 53.06 ± 0.04 โดยมีความ
เข้มข้นของโทลูอีนเท่ากับ 685 มิลลิกรัมต่อลูกบาศก์เมตร ที่อุณหภูมิ 175 องศาเซลเซียส และ 2)
ระบบสมดุล อุณหภูมิที่ทำการศึกษาอยู่ในช่วง 25 – 275 องศาเซลเซียส โดยกำหนดความเข้มข้นของ
โทลูอีน 685 มิลลิกรัมต่อลูกบาศก์เมตร พบว่าค่าร้อยละการกำจัดโทลูอีนสูงสุดเท่ากับ 87.11 ± 0.15
ที่อุณหภูมิ 275 องศาเซลเซียส และเริ่มพบก๊าซคาร์บอนไดออกไซด์ที่อุณหภูมิ 175 องศาเซลเซียส
ปริมาณก๊าซคาร์บอนไดออกไซด์จะเพิ่มขึ้นเมื่อเพิ่มอุณหภูมิปฏิกิริยา

สาขาวิชา ปิโตรเคมีและวิทยาศาสตร์พอลิเมอร์ ลายมือชื่อนิสิต ปิยธิดา แสงห้วยไผ่
ปีการศึกษา 2552 ลายมือชื่อ อ.ที่ปรึกษาวิทยานิพนธ์หลัก
ลายมือชื่อ อ.ที่ปรึกษาวิทยานิพนธ์ร่วม

5072358023 : MAJOR PETROCHEMISTRY AND POLYMER SCIENCE

KEY WORD : NANOGOLD / SILICA / TOLUENE / ADSORPTION / OXIDATION

PIYATHIDA SANGHUAYPAI: NANOGOLD SUPPORTED ON AMIDO-AMIDOXIME FUNCTIONALIZED SILICA FOR ADSORPTION AND CATALYTIC OXIDATION OF TOLUENE. THESIS ADVISOR: ASST.PROF. APICHAT IMYIM, Ph.D., THESIS CO-ADVISOR: ASST.PROF. SOAMWADEE CHAIANANSUTCHARIT, Ph.D., 77 pp.

Nanogold supported on amido-amidoxime functionalized silica (Au-Ami-SiO$_2$) was prepared by a simple mixing of amido-amidoxime functionalized silica in HAuCl$_4$ solution. Au-Ami-SiO$_2$ was characterized by X-ray diffraction (XRD) technique and surface area analyzer. Toluene vapor adsorption on Au-Ami-SiO$_2$ was studied. The adsorption capacity was measured by a fixed bed system at ambient temperature using argon as carrier gas. The effects of contact time, flow rate and adsorbent dose on adsorption capacity were investigated. Adsorption capacity increased with increasing of contact time, and decreased with the increase in flow rate and adsorbent dose. The maximum adsorption capacity of 1.36 g g^{-1} was obtained at 45 min contact time, 40 mL min^{-1} flow rate and 0.05 g of adsorbent. Catalytic oxidation of toluene vapor using Au-Ami-SiO$_2$ was investigated under air atmosphere. The effects of reaction temperature and toluene concentration were investigated in two systems; (i) in the continuous system, reaction temperature and toluene concentration were studied in the range of 25 – 175 °C and 190 – 685 mg m^{-3}, respectively. The highest percentage removal was 53.06 $\pm$ 0.04 % at 685 mg m^{-3}, at 175 °C and (ii) in the equilibrium system, the oxidation temperature was studied in the range of 25 – 275 °C with toluene concentration fixed at 685 mg m^{-3}, the highest percentage removal was 87.11 $\pm$ 0.15 % at 275 °C. CO$_2$ appeared firstly at 175 °C and increased when the reaction temperature increased.

Field of Study: Petrochemistry and Polymer Science   Student's Signature Piyathida Sanghuaypai

Academic Year: 2009   Advisor's Signature

                                                          Co-Advisor's Signature

ACKNOWLEDGEMENTS

CONTENTS

LIST OF TABLES

Table **page**

ศูนย์วิทยทรัพยากร

จุฬาลงกรณ์มหาวิทยาลัย

LIST OF FIGURES

LIST OF ABBREVIATIONS

BET	Brunauer-Emmett-Teller method
°C	Degree Celsius
EA	Elemental analysis
FID	Flame ionization detector
FT-IR	Fourier transforms infrared spectroscopy
g	Gram
$g\ g^{-1}$	Gram per gram
μg	Microgram
GC	Gas Chromatography
i.d.	Internal diameter
IUPAC	The international union of pure and applied chemistry
$mg\ L^{-1}$	Milligram per liter
mL	Milliliter
nm	Nanometer
q	Adsorption capacity
TEM	Transmission electron microscopy
XRD	X-ray diffractometry
SiO_2	Silica gel
$AP\text{-}SiO_2$	Aminopropyltriethoxysilane functionalized silica
$CA\text{-}SiO_2$	Cyano-amido functionalized silica
$Ami\text{-}SiO_2$	Amido-amidoxime functionalized silica

CHAPTER I

INTRODUCTION

1.1   Statement of the Problem

Nowadays, air pollution is a serious environmental problem. The effect of toxic air pollution increases by emission of air pollutants into the atmosphere caused by the industrial developments. Volatile organic compounds (VOCs) are recognized as major air pollutants emitted from resin manufacturing industry, petrochemical industries, refinery, including transportation activities, painting, coating and chemicals *etc*. [1]. VOCs are toxic and carcinogenic substances such as benzene, toluene and xylene *etc*.

Toluene is a volatile organic compound and widely used in many industries as a solvent. It is released from indoor and outdoor air into the environment. The central nervous system is the primary target organ for toluene toxicity in both humans and animals for acute (short-term) and chronic (long-term) exposures [2]. Therefore, toluene removal is important for the prevention of human health.

The presence of VOCs in air emissions is one of the problems concerned. Several methods have been used to remove them from air including thermal oxidation, catalytic oxidation, adsorption, absorption, condensation, bio-filtration and membrane separation. Among these methods, catalytic oxidation is an effective way for reducing the amount of VOCs [3].

Catalytic oxidation is one of the most promising technologies for the elimination of VOCs, because VOCs can be oxidized over a catalyst at temperature much lower than those of thermal oxidation or combustion. The energy is saved and the obtained product is less toxic or non-toxic such as H_2O and CO_2 [4]. The widely

used catalysts are supported noble metal (Pt, Pd, Rh) or metal oxide (Cu, Cr, Mn) *etc* [5].

Adsorption is the next most favoured technique for VOCs removal. It has good removal (recovery) efficiency, easy operation and low cost [6]. The general adsorbents were used in industries such as activated carbon and zeolite [3]. Moreover, silica was selected to be an adsorbent in many reports [7- 9].

Recently, gold catalysts have been successfully employed in many catalytic reactions, such as hydrogenation of carbon oxide and hydrocarbons, NO reduction, hydrochlorination of ethylene and the oxidation of VOCs [10]. Many reports presented the removal of VOCs using gold nanoparticles or nanogold supported on various metal oxides such as Au/Fe_2O_3 [11- 13], Au/CeO_2 [5], Au/Al_2O_3 [10, 14] and Au/TiO_2 [15], which can oxidize VOCs efficiently, as catalyst. It was found that gold nanoparticles or nanogold are better catalyst than bulk gold [16, 17].

However, the gold nanoparticles supported on silica solid support have not been reported as the adsorbent and the catalyst for VOCs removal. Therefore, in this research, gold nanoparticle supported silica gel was investigated for the removal of VOCs on the adsorption process and the catalytic oxidation. Toluene was chosen as a model molecule of VOCs.

1.2   Objectives of the thesis

1.2.1   To prepare gold nanoparticle supported silica gel.

1.2.2   To study parameter affecting the removal efficiency of toluene in air using gold nanoparticles as adsorbent and catalyst.

1.3   Scope of the thesis

The scope of the thesis can be summarized as following:

1.3.1   To synthesize amido-amidoxime functionalized silica.

1.3.2   To prepare gold nanoparticles and to characterize by X-ray diffraction spectroscopy (XRD) and surface area analyzer.

1.3.3   To study the adsorption efficiency of nanogold towards toluene in air by varying the following parameters: contact time, flow rate and adsorbent dose.

1.3.4   To study catalytic performance of nanogold for oxidation of toluene by varying the following parameters: temperature and toluene concentration.

1.4 The benefits of this thesis

The bifunctional (adsorbent and catalyst) nanogold supported silica for toluene vapor removal was obtained.

CHAPTER II

THEORY AND LITERATURE REVIEW

2.1   Properties of gold

Gold, (symbol Au) is an invaluable metal. The electronic configuration of gold is [Xe] $4f^{14}5d^{10}6s^{1}$ and it belongs to group IB of the periodic table [18]. It is generally found in nature as metallic gold and gold compounds. Gold is found in oxidation state from   -1 to +5 [19]. List of some physical properties of gold is shown in Table 2.1.

Table 2.1   Physical Properties of gold

Properties	*Value*
Phase	solid
Atomic weight (g/mol)	196.97
Atomic number	79
Density (g/cm^3)	19.3
Boiling point ($^{\circ}$C)	2856
Melting point ($^{\circ}$C)	1064
Electrical resistivity ($\mu\Omega$ cm) at 20°C	2.35
Electronegativity	2.4

Metallic gold is the most noble of the noble metals which is not react with oxygen, sulfur, or selenium at any temperature [20].

2.1.1 Bulk gold

Bulk gold has a soft, yellow color, bright luster and stability in air. It is ductile metal and is generally alloyed to strengthen it. The melting point of bulk gold is 1064 $^{\circ}$C. Bulk gold is characterized by high density, high electrical and thermal conductivity leading to widespread use in several aspect.

2.1.2 Gold in nanoscale

The color of gold nanoparticles may range from red through purple to blue and almost black due to a change in their absorption spectrum on the formation of aggregates. The colors shown appear to depend on the support used as well as on gold concentration, morphology, size and size distribution [21]. A melting point of gold nanoparticle is drawn from that of bulk gold. The reason for this phenomenon is the huge increase in surface area of gold nanoparticles. It is important to draw a distinction between the properties of gold in bulk form and those properties it exhibits when present in the form of tiny nanoparticles. The unique properties of gold at nanoscale finds application in a wide variety of areas, including colloids for biomedical marking, catalysts in chemical processing and pollution control [18].

2.1.3 Crystal structure and morphology

Bulk gold crystallizes in the face-centred cubic (fcc) habit which is closest-packed. Naturally-occurring macro-crystals of native gold exhibit the highly symmetrical cubic, octahedral or rombododecahedral crystal forms associated with this crystal structure [22]. Nevertheless, there is consideration and even confusion in the literature regarding the structure and external form of nano-particles of gold [23],

arising no doubt from the difficulties inherent in trying to physically characterize such tiny objects. As a result, several endeavors have been made to predict the structure of gold nanoparticles using molecular dynamics or other calculations. However, there is not yet complete agreement between the results of the calculations and of the experimental measurements, with conflicting claims being made for icosahedral or decahedral quasi-crystal structure, amorphous structure, or octrahedra, cuboctahedra and truncated octahedral based on fcc packing. Some shapes of gold nanoparticles are shown in Figure 2.1 [24].
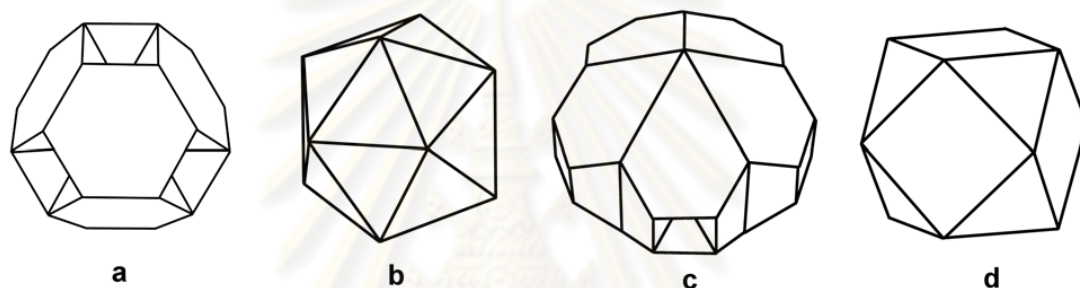
Figure 2.1   Comparison of (a) truncated octahedron, (b) icosahedron, (c) Marks decahedron and (d) cuboctahedron [24].

The nano-crystalline structure of gold diverges from the bulk gold. Several attempts have been made to predict the structure of gold nanoparticles by calculation. Usually, the results from calculations are not completely in agreement, either with is other or with the results of experimental techniques.

2.2   Catalytic properties of gold

Gold is traditionally regarded as being the least useful of the noble metals for catalytic purposes. However, the advent of nanoparticulate gold on high surface area oxide supports has demonstrated its high catalytic activity in many chemical reactions

such as   Haruta *et al.* recently discovered that supported gold nanoparticles are extremely catalytically active for carbon monoxide (CO) oxidation at temperatures much lower than room temperature when the gold particle size is below 5 nm [25, 26]. Many of reaction being studies will lead to new application areas for catalysis by gold in pollution control, chemical processing, sensors and fuel cell technology.

2.3   Preparation of gold nanoparticle

Gold nanoparticles could be prepared in aqueous solution by the chemical reduction. Furthermore, gold nanoparticles could be also prepared by photochemical reaction and other methods [27].

2.3.1 Chemical reduction

Gold nanoparticles preparation was prepared from substance in both solid and solution forms. The reaction between the substances and Au(III) is often a redox reaction which changes the oxidation state of gold from 3 to 0 (gold nanoparticle). Two main chemical reduction processes are summarized as follows.

2.3.1.1 Use of reducing agents

The reducing agents have been utilized for the reduction of Au(III) to gold nanoparticles. General reducing agents for the preparation of gold nanoparticles are $NaBH_4$ [28], citrate salts [29], ascorbic acid [30], hydroxylamine [31]. Alternatively, other reducing agents can be used such as tetrakis(hydroxymethyl)phosphonium chloride (THPC) [32] and borohydride [33, 34].

(a) Citrate reduction

Among the general methods of preparation of gold nanoparticles by reduction of gold(III) derivatives, the most popular one has been that using citrate reduction of HAuCl$_4$ in water, which was introduced by Turkevitch in 1951 [35]. The sodium citrate first acts as a reducing agent. Backward, the negatively-charged citrate ions are adsorbed onto the gold nanoparticles, introducing the surface charge that repels the particles and prevent them from aggregation [36]. This method is very often used even now when a rather loose shell of ligands is required around the gold core in order to prepare a precursor to valuable gold nanoparticle-based materials [37].

(b) The Brust-Schiffrin method

The stabilization of gold nanoparticles was reported by Mulvaney and Giersig in 1993, who showed the use of thaiols in different chain lengths. The technique of synthesis used thiol ligands that strongly bind with gold(0) due to the soft character of both Au and S [38, 39]. AuCl$_4^-$ from aqueous phase is transferred onto toluene phase using tetraoctylammonium bromide as the phase-transfer reagent and reduced by NaBH$_4$ in the presence of dodecanethiol.

2.3.1.2 On solid reduction

An on-solid reduction method is a method that involves the reduction of Au(III) by a solid containing reducing functional group. A solid support functionalized with a reducing group was investigated by Lin *et al* [10]. The functionalized polyacrylonitrile (PAN) with amidoxime group and then this product was subject to reduce Au(III) into gold nanoparticles. Moreover, the advantages of amidoxime group on solid support are that (i) there is an adsorption of gold nanoparticles, (ii) the solid

support acts as the stabilizer for preventing of agglomeration of gold nanoparticles and (iii) the preparation step of nanogold was shortened.

2.3.2 Photoreduction

In this method, gold nanoparticles are prepared by light source. However, it is not as extensive method as the chemical reduction method, because time required but it has advantages that the controlled reduction of metal ions can be carried out without using excess reducing agent, and no adsorbing contamination on the product occurs in the preparation process. Moreover, the radiation is absorbed regardless of the presence of light-absorbing solutes and products and the reduction reaction arises uniformly in the solution. Moriguchi et al. [40] used dioctadecyldimethylammonium chloride ($DODMA^+Cl^-$) to form complex with $AuCl_4^-$. The $DODMA^+AuCl_4^-$ complex was produced and exposed to UV-light for the preparation of gold nanoparticles. This photoreduction process lasted 12 hours.

2.3.3 Other methods

The seeding-growth procedure is another popular technique. Recent studies have well led to control of the size distribution in the range 5-10 nm, although the sizes can be manipulated by varying the ratio of seed to metal salt [41, 42, 43]. The step-by-step particle enlargement is more effective than a one-step seeding method to avoid secondary nucleation [44].

Using a solution-spray technique [45], an aqueous solution of $HAuCl_4$ and titanium tetrachloride was atomized by an ultrasonic device to produce a mist without separation of the components: this was then calcined, and the fine particles collected on a glass filter at the outlet. Samples of 1 wt. % Au/TiO_2 contained 4 nm particles when the spray reaction temperature was 673 K.

Moreover, the sonochemical techniques [46], gold particles can be deposited on the surface of supports by ultrasound, which induces chemical changes due to

cavitation phenomena caused by the formation, growth and implosive collapse of bubbles in a liquid [47]. Gold has been deposited on mesoporous silica in this way [48], the support being first immersed for three weeks in a water-*iso*propanol solution of $HAuCl_4$ to equilibrate the concentrations of the reagents throughout the pores: the support turned purple during sonication. Radicals formed from the *iso*propanol may also have participated in the reduction, which was faster in the pores than in solution, and gave smaller particles (5.2 nm) than in solution (20-30 nm) in the absence of support.

2.4   Application of gold nanoparticles

Many of the applications of gold are based on its unique properties. It is probable that gold will turn out to have a special catalytic chemistry of its own, comprising both heterogeneous and homogeneous aspects, and leading to appropriate applications [49].

Gold is used in a wide range of industrial and medical applications. Recently, gold nanoparticle catalysts have been found to be active under mild conditions, even at ambient temperature or less, they are seen as having the potential to reduce the running costs of chemical plants and could increase the selectivity of the reactions involved where applicable.

In pollution control applications, such as air cleaning, low light-off autocatalysts and diesel oxidation catalysts have the purification of hydrogen streams used in fuel cells; heterogeneous gold catalysts have the characteristics to become the catalysts of choice. Table 2.2 lists such reactions, which usually take place at much lower temperatures or with higher degrees of selectivity over Au catalysts than other metal catalysts [50].

Table 2.2 Ongoing and potential applications of Au catalysts [50]

Field of application	*Reactants or Reactions*	*Support materials*
Indoor air quality control	odour (commercialized), CO Sick house gases	Fe_2O_3 TiO_2
Pollutant abatement	dioxin oxidation-decomposition NO reduction N_2O decomposition	Fe_2O_3 Al_2O_3 Co_3O_4
H_2 energy carrier	water-gas shift CO removal fuel cell anode	ZrO_2, CeO_2 Al_2O_3, Mn_2O_3, Fe_2O_3 Carbon black
Chemical process	hydrochlorination hydrogenation liquid-phase selective oxidation propylene oxidation	$AuCl_3$/ activated carbon ZnO activated carbon TiO_2 (anatase) and Ti-SiO_2

2.5   Volatile organic compounds (VOCs) in air

Volatile organic compounds (VOCs) are organic chemicals that easily vaporize to atmosphere at room temperature [51]. These compounds based on carbon chains or ring (and also containing hydrogen) and may contain oxygen, nitrogen and other elements. These were not consisting of carbon monoxide, carbon dioxide, carbonic acid, metallic carbides and carbonate salts [52]. VOCs often exist as vapors or liquids at room temperature but may also be in the form of solids. For most VOCs, air is the

main route of exposure. Common volatile organic chemicals and their sources are listed in Table 2.3.

Table 2.3 Common volatile organic chemicals and their sources [53]

Chemicals	*Major sources of exposure*
Acetone	Cosmetic
Alcohols (ethanol, isopropanol)	Spirits, cleansers
Aromatic hydrocarbons (toluene, xylenes, ethylbenzene, trimethylbenzene)	Paints, adhesives, gasoline, combustion sources
Aliphatic hydrocarbons (octane, decane, undecane)	Paints, adhesives, gasoline, combustion sources
Benzene	Smoking, auto exhaust, passive smoking
Carbon tetrachloride	Fungicides, global background
Chloroform	Showering, washing clothes, dishes
p-Dichlorobenzene	Room deodorizers, moth cakes
Formaldehyde	Pressed wood products
Methyl chloride	Paint stripping, solvent use
Styrene	Smoking
Tetrachloroethylene	Wearing or strong dry-cleaned clothes
Trichloroethylene	Unknown (cosmetic, electronic parts)
Terpenes (limonene, α-pinene)	Scented deodorizers, polishes, food, fabrics

VOCs are usually grouped into methane (CH_4) and non-methane (NMVOCs). Methane is an extremely efficient greenhouse gas, its environmental impact principally related to its contribution to global warming. Within the NMVOCs, the aromatic compounds such as benzene, toluene and xylene are suspected carcinogens [54].

VOCs are emitted from various sources, both indoor and outdoor air. The main indoor sources are consumer products (e.g. room air deodorants), building materials (e.g. paints, adhesives) and personal activities (smoking, driving and taking showers). Exposure from outdoor sources such as chemical plants, petroleum refineries, automobiles, and hazardous waste sites appears to be low, accounting generally for no more than 25% of personal exposure [53].

The emission of VOCs in air is a serious environmental problem because they are harmful to plant, animal and human life. In general, short-term health effects of exposure to VOCs include eye, nose and throat irritation, and central nervous system responses such as dizziness, headaches and loss of short-term memory. Besides, long-term health effects may include cancer [53].

2.6   Information of toluene

Toluene, also known as toluol, methylbenzene and phenylmethane, is a colorless liquid with a sweet pungent odor and it evaporates quickly [55]. It is an aromatic hydrocarbon that is widely used as a mixture added to gasoline to improve octane ratings, to produce benzene and as a solvent in paints, coating, synthetic fragrances, adhesives, inks, and cleaning agents. Toluene is also used in the production of polymers to make nylon, plastic soda bottles and for pharmaceuticals, dyes, cosmetic nail products, and the synthesis of organic chemicals [2].

2.6.1   Properties of toluene

The structure and physical/chemical properties of toluene are shown in Figure 2.2 and Table 2.4, respectively.
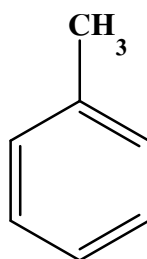
Figure 2.2   The chemical structure of toluene.

Table 2.4   Physical and chemical properties of toluene [56]

Properties	*Value*
Description	Colorless liquid
Molecular formula	C_7H_8
Molecular weight (g/mol)	92.13
Density (g/cm^3) at 20°C	0.8661
Boiling point (° C)	110.6
Melting point (° C)	-94.9
Vapor pressure (torr) at 25°C	28.1
Solubility	miscible in most organic solvents
Conversion factor (at 25°C)	1 ppm = 3.76 mg m^{-3}

2.6.2 Sources and potential exposure

Toluene occurs naturally as a component of crude oil and is produced from petroleum refining and coke oven operations. It is a major aromatic constituent of gasoline [57].

Inhalation is the primary route of toluene exposure. The highest concentrations of toluene usually occur in indoor air from the use of common household products such as paint, paint thinners, adhesives, synthetic fragrances and nail polish and cigarette smoke [53]. Evaporation of gasoline and automobile exhaust are the principal sources of toluene to the ambient air and toluene may also be released to the ambient air during the production, use, and disposal of industrial and consumer products that contain toluene.

Levels of toluene measured in rural, urban, and indoor air averaged 1.3, 10.8, and 31.5 micrograms per cubic meter ($\mu g/m^3$), respectively [2].

Effect of toluene can occur from accidental or deliberate inhalation of fumes, ingestion or absorption through the skin. In the case of inhalation, toluene is rapidly distributed to the more vasculated tissues such as the liver and brain [53]. Toluene is a central nervous system (CNS) depressant which means it can decreased rate of breathing, heart rate, and mental capacity [55]. The regulatory and advisory values for exposure of toluene were shown in Table 2.5 [2].

Table 2.5 Regulatory and advisory values for exposure of toluene [2]

Government regulations	Regulatory, advisory numbers [a] (mg/ m^3)
AIHA ERPG-1, ACGIH TLV	188
NIOSH REL	375
NIOSH STEL	560
OSHA PEL	754
AIHA ERPG-2, OSHA ceiling	1130
NIOSH IDLH	1885

[a] Regulatory number are values that have been incorporated in Government regulation, while advisory number are nonregulatory values provided by the Government or other groups as advice. OSHA numbers are regulatory, where as NIOSH, ACGIH, and AIHA numbers are advisory.

AIHA ERPG: American Industrial Hygiene Association's emergency response planning guidelines. ERPG-1 is the maximum airborne concentration below which it is believed nearly all individuals could be exposed up to one hour without experiencing other than mild transient adverse health effects or perceiving a clearly defined objectionable odor; ERPG-2 is the maximum airborne concentration below which it is believed nearly all individuals could be exposed up to one hour without experiencing or developing irreversible or other serious health effects that could impair their abilities to take protective action.

ACGIH TLV: American Conference of Governmental and Industrial Hygiene's threshold limit value

NIOSH REL: National Institute of Occupational Safety and Health's recommended exposure limit

NIOSH STEL: NIOSH's recommended short-term exposure limit

OSHA PEL: Occupational Safety and Health Administration's Permissible exposure limit

OSHA ceiling: OSHA's Permissible exposure limit ceiling value

NIOSH IDLH: NIOSH's immediately dangerous to life or health concentration

2.7   VOC removal techniques

Many different techniques are used to control VOCs emissions. These techniques are classified into two different groups: In the first group, control of VOCs emissions is achieved by modifying the process equipment, raw material, and/or change of process, while in the other class an additional control method has to be adopted to regulate emissions. Though the former is the most effective and efficient method, its applicability is limited, as generally it is impossible to improve the process and/or the equipment. The techniques in the second group are add-on-control techniques, further classified into two sub-groups, namely the destruction and the recovery of VOCs. An organizational tree diagram showing various VOC control techniques is presented in Figure 2.3 [58].
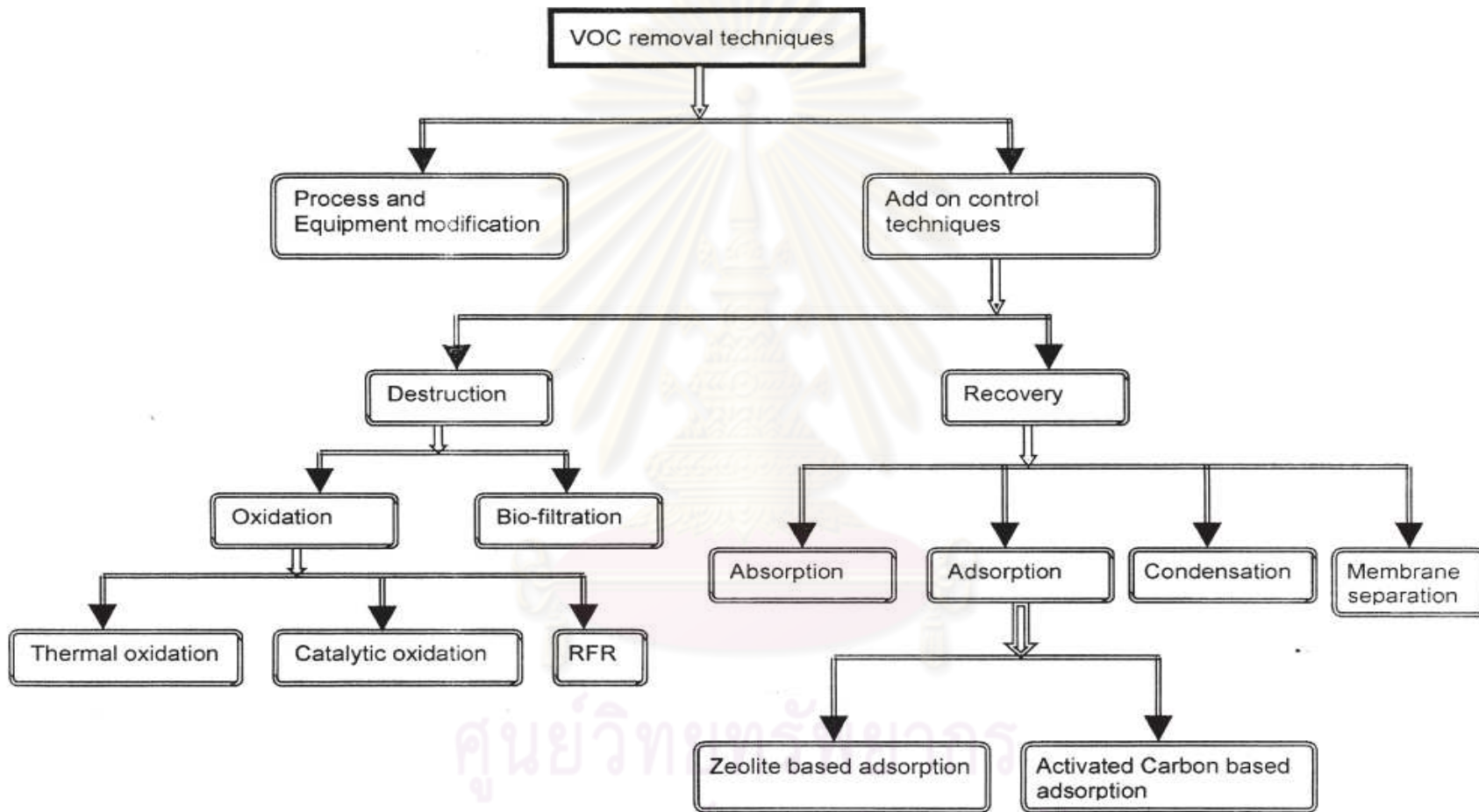
Figure 2.3   Classification of VOC control techniques [58]

VOCs are destroyed by different types of oxidation such as thermal and catalytic, and digestion of VOCs under aerobic conditions by microbes (Bio-filtration). Several techniques for recovery of VOCs such as condensation, absorption, adsorption and membrane separation are discussed here in detail.

2.7.1 Thermal oxidation

Thermal oxidation is the process of oxidizing combustible materials by rising their temperature above the auto ignition point in the presence of oxygen and maintaining it at a high temperature for sufficient time to complete combustion to carbon dioxide and water [59]. Available with thermal energy recovery options to reduce operating costs, thermal oxidizers are very popular [58].

Thermal oxidation is a proven method for destroying VOCs. Thermal oxidizer can be used to reduce emissions from almost all VOC sources, including process vents, storage tanks, material transfer operations, treatment, storage and disposal facilities, surface coating operations and vessel cleaning operations [58].

2.7.2 Catalytic oxidation

Catalytic oxidizers operate similarly to thermal oxidizers. The catalyst is always a noble metal such as palladium or platinum (other metals are used, including Cr, Mn, Cu, Co, and Ni) entrusted on an alumina support [60]. The primary difference is that the gas, after passing through the flame area, passes through a catalyst bed. The catalyst has the effect of increasing the oxidation reaction rate, allowing the reaction to appear at a lower temperature than that is required for thermal oxidation. The catalytic system is well suited to low concentration operations or those that operate in a cyclic manner. They are often used for vent controls where flow rates and VOCs content are variable [59].

Oxidation reaction, oxygen and VOCs migrate to the catalyst surface by diffusion from the gas stream and are adsorbed onto the active sites on the catalyst surface, where oxidation occurs. The products of oxidation reaction are then adsorbed from the active sites by the gas [59]. The oxidation reaction is shown in equation 2.1

$$C_xH_yO_z + \left[x + \frac{y}{4} - \frac{z}{2}\right]O_2 \xrightarrow[\triangle]{catalyst} xCO_2 + \frac{y}{2}H_2O \qquad (2.1)$$
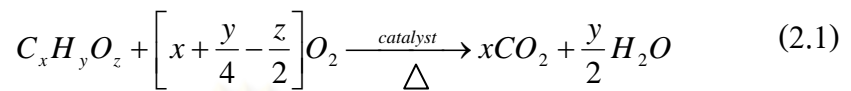
Catalytic oxidizers are able to reduce the emission from many VOC sources, including process vents, gasoline bulk-loading operations and solvent evaporation processes [59].

2.7.3 Bio-filtration

Bio-filtration is a process in which polluted air is passed through a porous packed medium that supports a growing population of micro-organisms. The contaminants are first adsorbed from the air to the water/bio-film phase of the medium. The degree of adsorption is a function of the chemical characteristics of the specific contaminant (water solubility, Henry's constant, and molecular weight). Once the contaminants are adsorbed, the micro organisms change them to carbon dioxide, water, inorganic products and bio-mass [61, 62].

2.7.4 Condensation

Condensation is the process of converting a gas or vapor to liquid. Any gas can be reduced to a liquid at lowering its temperature and/or increasing its pressure. The basis approach is to reduce the temperature of the gas stream, but increasing the pressure of a gas can be expensive [60].

2.7.5 Absorption

Absorption is used to remove VOCs from gas streams by liquid solvent. Any soluble VOCs will transfer to the liquid phase. In effect, the air steam is scrubbed. This takes place in an absorber tower designed to provide the liquid vapor contact area necessary to facilitate mass transfer. Using tower packing and trays as well as liquid atomization can provide this contact [58].

2.7.6 Adsorption

Adsorption as applied to air pollution control is the process by which organic molecules in a gas stream are retained on the surface of solid particles [63]. The gas molecules being removed are referred to as the *adsorbate*, while the solid doing the adsorbing is called the *adsorbent*. Adsorbents are highly porous particles. Several materials are used effectively as adsorbing agents. The most typical adsorbents used in industry are activated carbon, silica gel, activated alumina (alumina oxide), and zeolites (molecular sieves) [60].

The adsorption process is grouped into two types, namely, physical adsorption and chemisorption based on the interaction between adsorbate and adsorbent which is shown in Figure 2.4 [60]. Chemisorption involves chemical bonding and is irreversible [60]. Physical adsorption occurs when organic molecules are held on the surface and in the pores of the adsorbent by the weak Van der Waals force of interaction and is widely characterized by low heat of adsorption, and by the fact that the adsorption equilibrium is reversible and fast established [58]. Physical adsorption has been found to be more significant in the case of separation processes which are used completely in air pollution control systems.

Step 1: diffusion to
adsorbent surface

Step 2: migration into
pores of adsorbent

Step 3: monolayer
buildup of adsorbate

Contaminant molecules
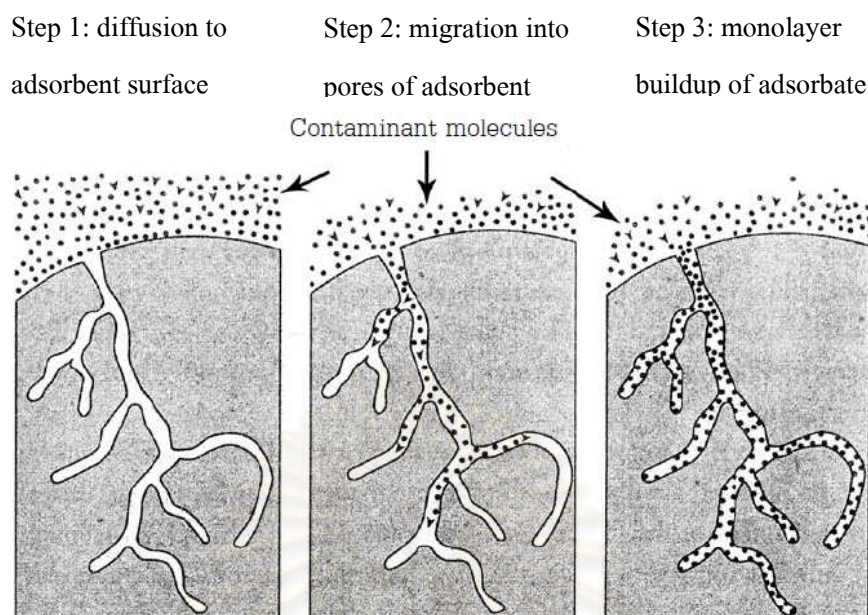
Figure 2.4 Mechanism of Adsorption [60].

2.7.7 Membrane separation

In a general membrane separator, the waste gas stream is fed to an array of membrane modules, where organic solvent preferentially permeates the membrane. The organics in the permeate stream are then condensed and remove as a liquid for recycle or recovery. The purified gas stream is removed as the residue. Moving through the membrane is induced by maintaining the vapor pressure on the permeate side of the membrane lower than the vapor pressure on the feed side.

Most membranes are made from synthetic polymers; however, some vendors are considering inorganic materials, such as ceramics, to deal with more rigorous applications [59].

There are several methods for abating VOC emissions in the air pollution control. The major advantages and disadvantages of their performances are listed in Table 2.6.

Table 2.6 Advantages and disadvantages of VOCs abatement in air pollution control [60, 63]

Techniques	Advantage	Disadvantage
Thermal oxidation	- simplicity of operation - capability for high destruction efficiency of organic contaminants	- requires a high operating temperature. - relatively high operating costs
Catalytic oxidation	- higher destructive efficiency at lower temperature as compared to the thermal combustion - can reduce the amount of pollutants from combustion, the complete combustion products are desirable - have a potential saving in fuel costs	- more expensive for the catalyst - have some limited application for liquid and not applicable for solid wastes disposal
Adsorption	- product recovery may be possible - capability to remove gaseous or vapour contaminants from process stream to extremely low levels	- adsorbent progressively deteriorates in capacity as the number of cycles increases - adsorbent regeneration requires a stream or vacuum source
Absorption	- capable of achieving relatively high mass-transfer efficiencies - ability to collect particulars as well as gases	- may create water (or liquid) disposal problem - product collected wet

Table 2.6 Advantages and disadvantages of VOCs abatement in air pollution control (continued) [60, 63]

Techniques	*Advantage*	*Disadvantage*
Condensation	- pure product recovery - water used as the coolant in and - indirect contact condenser dose not contact the contaminated gas stream and can be reused	- relatively low removal efficiency for gaseous contaminants - coolant requirements may be extremely expensive
Biofiltration	- requires less initial investment - less non-harmful secondary waste	- slow - selective microbes decomposes selective organics - no recovery of material
Membrane separation	- useful for treating vent gases that are difficult to treat by using conventional processes - recovery of solvent may offset the operating costs	- have a temperature limitation for organic polymeric membranes - membranes are rare and costly

Catalytic oxidation is the most commonly used technique, though it destroys the valuable VOCs. Further, the oxidation process with lower temperature is a good economical option. It may also generate toxic combustion products, which need further processing. These limit its applicability. Catalytic combustion is a good alternative that overcomes some of its limitations.

Adsorption is the next most favored technique. It has good removal (recovery) efficiency, though it requires higher capital investment and operating costs. Desorption of adsorbent and separation of VOCs from desorbed solution increase the complexity

and cost of the process. There are many solvent recovery units available commercially based on the adsorption principle.

From the advantage of two techniques, the prepared Au-Ami-SiO$_2$ was separated into two parts, the first part: SiO$_2$ was high surface area support and the second part: gold could boost oxygen atom to react with toluene on surface. Both advantages appeared in Au-Ami-SiO$_2$, so adsorption and catalytic oxidation were chosen to study in this work.

Since the pioneering work on Au catalysts by Haruta [64], many studies of gold catalysts and gold-supported catalysts (including Fe$_2$O$_3$, Co$_3$O$_4$, TiO$_2$, and Mn$_2$O$_3$) for VOCs oxidation have been reported. Au/Fe$_2$O$_3$ [11, 12, 13], Au/CeO$_2$ [5], Au/Al$_2$O$_3$ [10, 14] and Au/TiO$_2$ [15] have high activities for decomposition of different kinds of VOCs. In the case of gold supported on ferric oxide could increase the mobility of the lactice oxygen to oxidation reaction [11, 13], which could completely oxidize toluene at 400°C [11]. Other researchers concluded that gold metal was more efficiency than silver metal and copper metal on ferric oxide, respectively [13]. For Au/CeO$_2$, gold caused decreasing in strength of Ce-O bonds adjacent to gold atoms, thus activating the surface capping of oxygen [5] which involved in Mars-van Krevelen reaction mechanism [5, 11, 13], toluene conversion started at about 200 $^\circ$C and 100 % was achieved at 360 $^\circ$C by deposition-precipitation method [5]. For Au/CeO$_2$/Al$_2$O$_3$ and Au/Al$_2$O$_3$ catalysts, they could completely oxidize benzene at 300°C and lower in Au/Fe$_2$O$_3$ system [10]. Then oxidation benzene was used Au/TiO$_2$ as catalyst, which could completely oxidize benzene at 350°C. Particle size and amount of nanogold particle affected catalytic efficiency [65]. Catalytic performance of nanosized Pt-Au alloy catalyst in oxidation of methanol and toluene, the catalyst was efficiency oxidize to toluene [66]. Recently, the effect of gold added to palladium supported on a new mesoporous (TiO$_2$) for total oxidation of volatile organic compounds was studied. It was found that completely oxidized toluene at 220°C [15].

According to the previous researches, it could conclude that gold nanoparticles on metal oxide (Fe, Ce, Al, Zn and Ti) support exhibit a good capability in catalytic VOCs oxidation especially for toluene.

General adsorbents have high specific surface area, small pores (micropore and mesopore) responsible for adsorption. The adsorbents for VOCs removal were continuously developed in many previous researches. The maximum toluene adsorption capacity of mesoporous silica [67], zeolite [68], activated carbon [69], MCM-41 [70] and silica [7] was 0.0013, 0.0049, 0.0059, 0.0066 and 0.0119 mol g^{-1}, respectively. From the literatures, silica was a good adsorbent for toluene adsorption.

From both advantages of gold and silica mentioned in the previous paragraph, the VOCs removal on gold nanoparticles supported on silica was investigated in this study. Silica was chosen because of the cheap and easy chemical modification. Since functional groups of amidoxime have reducing-adsorption capacity and selectivity towards Au(III) ion [6], amidoxime silica was previously developed in our research unit (Figure 2.5) and then used to reduce gold ions to gold nanoparticles. In this research, we are interested in applying gold nanoparticles on silica support for removal of VOCs. Toluene was chosen as a model molecule of VOCs.
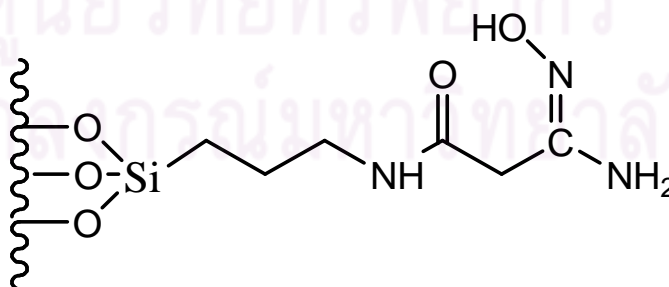
Figure 2.5 Structure of amido-amidoxime functioalized silica.

CHAPTER III

EXPERIMENTAL

3.1   Chemicals

In this thesis, all chemicals used were of analytical grade listed in Table 3.1.

Table 3.1   Chemical list

Chemicals	Suppliers
Air zero 99.99%	Praxair
Argon gas 99.99%	Praxair
(3-aminopropyl)triethoxy silane	Fluka
Calcium hydride	Fluka
Dichloromethane	ZEN POINT
Ethanol	MERCK and U & V holding Thailand
Gold(III) standard solution (1000 mg L^{-1})	MERCK
Hydrochloric acid 37%	MERCK
Hydroxylamine hydrochloride	MERCK
Methyl cyanoacetate	Fluka
Potassium hydroxide	MERCK

Table 3.1 Chemical list (continued)

Chemicals	Suppliers
Sodium hydroxide	MERCK
Toluene	Fisher Scientific
Toluene standard solution (10 ng/μL)	Ehrenstorfer Quality

3.2 Instruments and Apparatuses

The instruments used in this study were listed in Table 3.2.

Table 3.2 List of analytical instruments

Analytical instruments	Manufacture : Model
1. Gas chromatograph (GC)	Varian : CP-3800
2. Gas chromatograph-Mass spectroscopy (GC-MS)	Varian : Saturn 2200
3. Surface area analyzer	BEL Japan : BELSORP-mini
4. X-ray diffractometer (XRD)	DMAX 2200/Ultima +(Rigaku)
5. Transferpipette : 100-1000 μL, 0-10 μL	Bran
6. Centrifuge	Sanyo : Centaur 2
7. Digital balance	Mettler : AT 200
8. Stirrer	Gem : MS 101
9. Stirrer/Hot plate	CORNING : PC-420 and PC-620
10. Glassware	-

Adsorption Apparatuses

The homemade apparatus for adsorption of toluene vapor in our laboratory comprises of a borosilicate tube reactor of 0.54 cm internal diameter and 11.0 cm reactor length, a gas-liquid saturator, an argon gas cylinder and Tedlar® bag. The apparatus was shown in Figure 3.1.

Catalytic Apparatuses

The homemade catalytic apparatus for oxidation of toluene in our laboratory comprises of a borosilicate tube reactor of 0.54 cm internal diameter and 11.0 cm reactor length, heating cables, a thermocouple connected to a temperature controller, a gas-liquid saturator, an air zero gas cylinder and Tedlar® bag. The catalytic apparatus was shown in Figure 3.2.
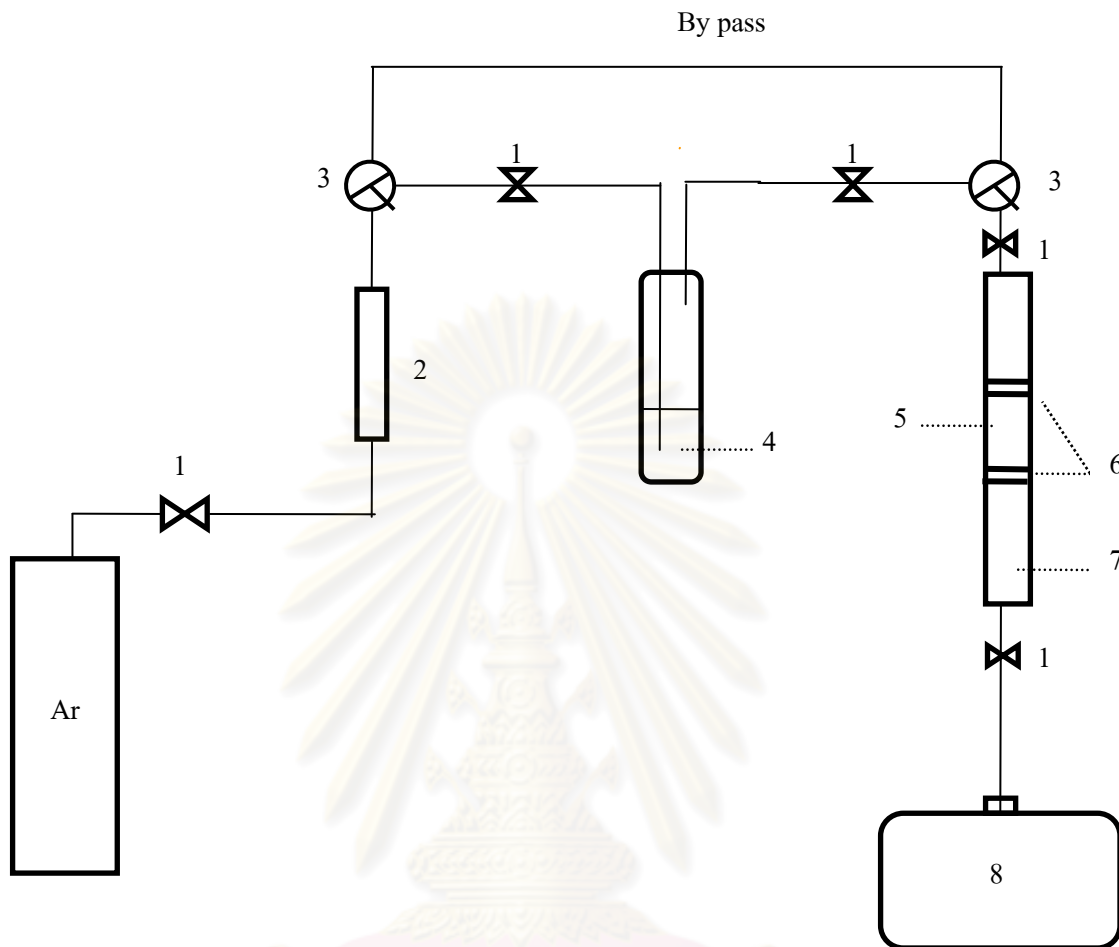
Figure 3.1　The apparatus for adsorption of toluene vapor.

(1)　needle valve　　　　(2)　rotameter

(3)　three way valve　　　(4)　toluene saturator

(5)　adsorbent　　　　　(6)　quartz wool

(7)　borosilicate tube reactor　(8)　Tedlar® bag
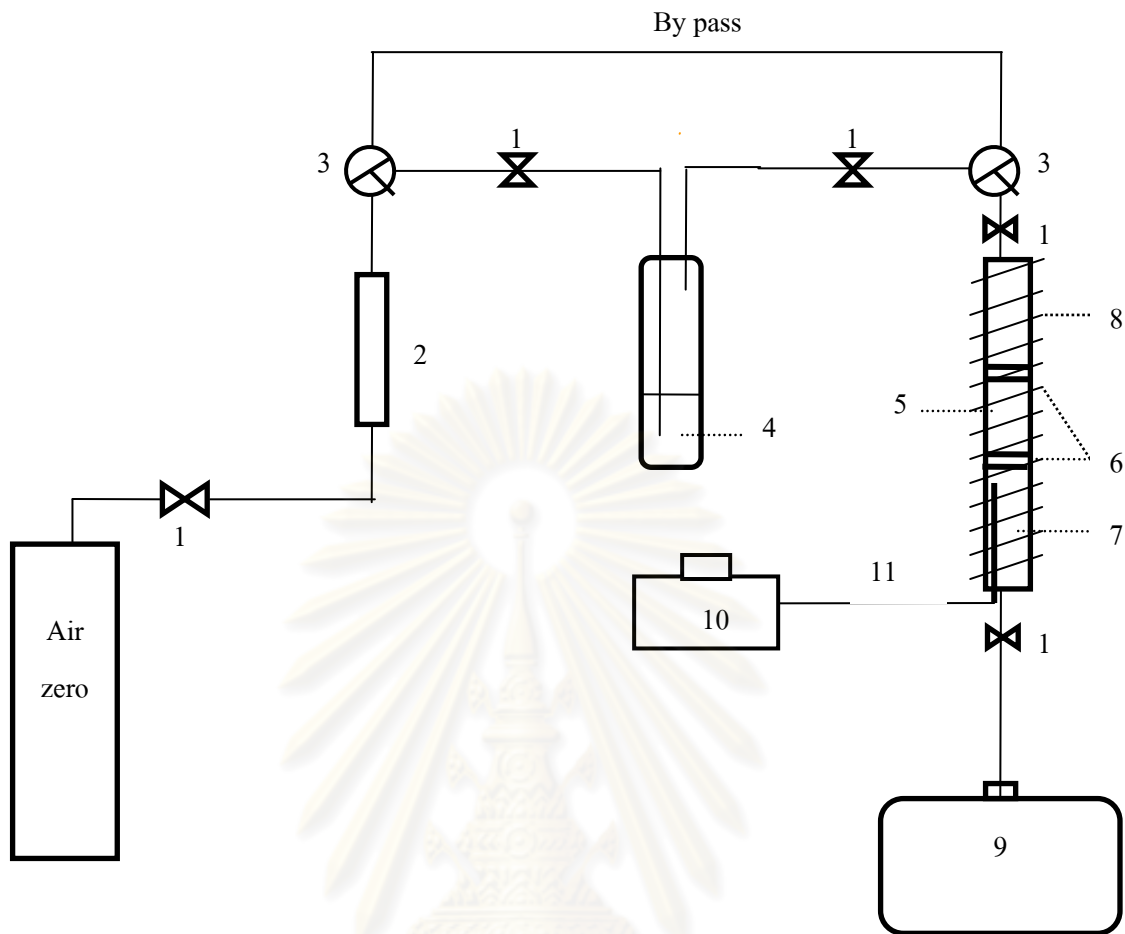
Figure 3.2   The apparatus for catalytic oxidation of toluene

(1) needle valve   (2) rotameter

(3) three way valve   (4) toluene saturator

(5) catalyst   (6) queartz wool

(7) borosilicate tube reactor (8) heating cables

(9) Tedlar® bag   (10) temperature controller

(11) thermocouple

3.3   Methodology

3.3.1   Preparation of reagents

a)   Dried toluene solution

Toluene and calcium hydride were added to a 1000 mL two-neck round bottom flask and refluxed under nitrogen atmosphere for 4 hours.

b)   Hydrochloric acid solutions

Hydrochloric acid solutions (1% v/v, 5% v/v and 1 M) for pH adjustment were prepared by subsequent dilutions from the concentrated solution.

c)   Sodium hydroxide solution

Sodium hydroxide solution (1 M) for pH adjustment of hydroxylamine solution was prepared by dissolving an appropriate amount of NaOH in deionized (DI) water.

d)   Potassium hydroxide solution

Potassium hydroxide solutions (1% w/v, 5% w/v and 1 M) for pH adjustment were prepared by dissolving an appropriate of KOH in DI water.

3.3.2 Preparation of gold nanoparticles on silica

a) Synthesis of amido-amidoxime functionlized silica.

The synthesis of amido-amidoxime functionalized silica was carried out in three steps according to the procedure proposed by our colleaques; Ngeontae *et al*. [71] as shown in Figure 3.3.
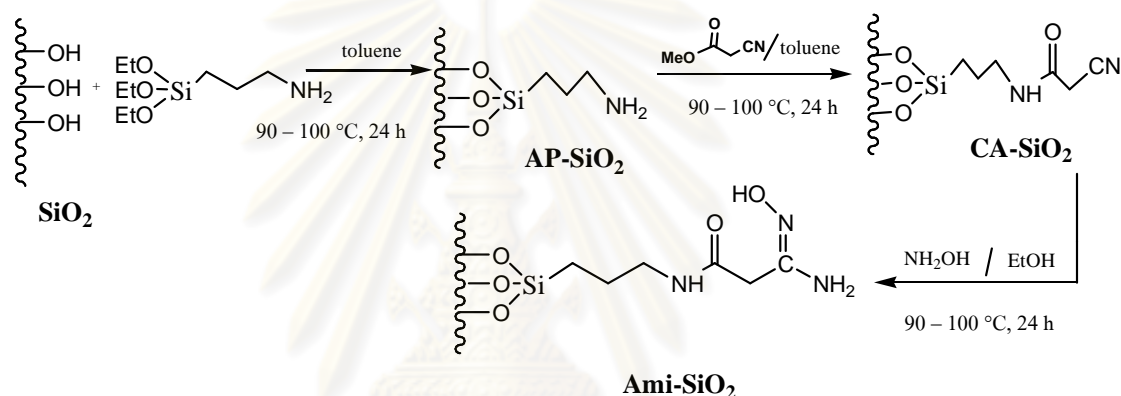
Figure 3.3 The synthetic pathway of Ami-SiO$_2$ [71].

Step 1: silica gel (25 g) in a 250 mL two-neck round bottom flask was refluxed with dried toluene at 90-100 °C under stirring and nitrogen atmosphere. After 1 hour (3-aminopropyl)triethoxysilane (10 mL) was added. The mixture was stirred for 24 hours under nitrogen atmosphere. The solid was filtered and washed with dichloromethane (3 × 200 mL). The product was designated as AP-SiO$_2$.

Step 2: AP-SiO$_2$ was refluxed with dried toluene at 90-100 °C for 1 hour. Then, 6.2 g of methyl cyanoacetate was added. This mixture was stirred for 24 hours in nitrogen atmosphere under reflux condition. The solid was filtered and washed with ethanol (3 × 100 mL) and dichloromethane (2 × 200 mL), respectively. The product was designated as CA-SiO$_2$.

Step 3: CA-SiO$_2$ was transferred to a 250 mL two-neck round bottom flask and ethanol and hydroxylamine solutions were added. The latter solution was prepared by mixing hydroxylamine hydrochloride (4.6 g) with sodium hydroxide (2.7 g) in DI water (75 mL) and the pH of the solution was adjusted to 7.0 with 1 M HCl and 1 M NaOH. The mixture was again refluxed at 78 °C for 24 hours under nitrogen atmosphere. The solid was filtered and washed with distilled water (3 × 200 mL), ethanol (2 × 200 mL), and dichloromethane (3 × 200 mL), respectively. The final product, amino-amidoxime silica (Ami-SiO$_2$) was kept in a desiccator box.

b) Preparation of gold nanoparticles

Gold nanoparticles were generally prepared by mixing 0.4 g of Ami-SiO$_2$ with 100 mL of Au (III) solution (40 mg Au/L). The pH of slurry was controlled at 3. The mixture was stirred for 30 minutes, and then centrifuged at 3000 rpm for 10 minutes. The resulting solid (Au-Ami-SiO$_2$) was separated and dried at approximately 100 °C for 2 hours [72].

3.4   Characterization of materials

XRD and Surface area analyzer were used for the characterization of gold nanoparticles.

3.4.1 X-ray driffraction (XRD)

The crystallite patterns of gold nanoparticles were determined. The diffraction pattern was recorded in the 2-theta ranged from 10-90 degree using a CuK α radiation (40 kV, 30 mA) equipped with a monochromator.

3.4.2 Surface area analyzer

The gold nanoparticles were analyzed for the specific surface area by nitrogen adsorption method using a BET model. The sample was weighed approximately 40 mg and pretreated at 400 °C for 3 hours before each measurement.

3.5 Adsorption study

The adsorption of toluene vapor by Au-Ami-SiO$_2$ was studied using a fixed bed system using the apparatus system as shown in Figure 3.1. The adsorbent (Au-Ami-SiO$_2$) was loaded into the borosilicate tubular reactor, with the inner diameter of 0.54 cm and held in place by a plug of quartz wool, the adsorbent was covered with small amount of quartz wool. Argon was used as a carrier gas. The gas flow rate was adjusted using a rotameter. Then, gas from a pressurized cylinder was flowed into the gas-liquid saturator previously filled with liquid toluene (0.4 mL). The feed of toluene vapor was passed from top through the adsorbent at ambient temperature. After time on stream, the effluent gas was collected in a Tedlar® bag. The concentration of toluene vapor was determined using a gas chromatograph (GC). The GC condition was shown in Table 3.3.

In this work, blank test was performed without adsorbent in the reactor, at the same condition.

Table 3.3 GC condition for measurement of toluene vapor concentration.

Parameter	Operating condition
Column	CP-sil5 (30 m × 0.25 mm)
Injector temperature (°C)	250
Column temperature (°C)	50
Column flow (ml min^{-1})	1.0
Carrier gas	N_2
Detector	Flame ionization detector (FID)
Injection volume (μL)	5

Moreover, the effect of contact time, flow rate and adsorbent dose were investigated in this work. All adsorption experiments were performed in duplicate.

3.5.1 Effect of contact time and flow rate

The effect of flow rates and contact times were investigated under the following conditions;

At a 40 mL min^{-1} flow rate, the contact times were studied at 15, 30, 45, 60 and 90 minutes.

At a 60 mL min^{-1} flow rate, the contact times were studied at 10, 20, 30, 40 and 60 minutes.

At a 80 mL min^{-1} flow rate, the contact times were studied at 7.5, 15, 22.5, 30 and 45 minutes.

The amount of adsorbent was fixed at 0.1 g. The method of adsorption was performed using the same procedure described in Section 3.5.

3.5.2 Effect of adsorbent dose

The amount of adsorbent was varied in a range of 0.05-0.2 g. The flow rate was fixed at 40 mL min^{-1} with varying contact times of 15, 30, 45 and 60 minutes. The reaction was performed using the same procedure described in Section 3.5.

3.6 Catalytic oxidation

3.6.1 Fixed bed system

The catalysis study was carried out using the apparatus shown in Figure 3.2. The catalyst (0.05 g) was loaded into the borosilicate tubular reactor and held in place by a plug of quartz wool, the catalyst portion was covered with a small amount of quartz wool. Air zero, with a purity of 99.99% was used as carrier gas. The temperature of reactor was controlled to constant. At the same time air was flowed for 1 hour in order to equilibrate the catalyst. The gas flow rate was adjusted using the rotameter and set to 40 mL min^{-1}. Then, air from a cylinder was flowed into the saturator, previously filled with liquid toluene (0.4 mL). The feed of toluene vapor in air was passed from top through the catalyst at a reaction temperature. After time on stream of 45 minutes, the effluent gas was collected in a Tedlar® bag. The concentration of toluene vapor was determined using the GC with the condition shown in Table 3.3.

In this work, blank test was performed without catalyst in the reactor, at the same condition. All catalytic experiments were performed in duplicate.

Parameters affecting the reaction were studied as follows:

3.6.1.1   Effect of temperature

The effect of temperature was studied by varying the temperatures of 25, 75, 125 and 175 °C. The experiment was performed in the similar way to that described in Section 3.6.1.

Moreover, pure silica was also used as a control for the study of the effect of temperature in the same manner of Au-Ami-SiO$_2$.

3.6.1.2   Effect of toluene concentration

The effect of toluene concentration was studied by varying the amount of liquid toluene of 0.1, 0.2, 0.3 and 0.4 mL. The experiments were set up at the reaction temperature of 175 °C. The reaction was performed in the similar way to that described in Section 3.6.1.

In addition, pure silica was also used as a control for the study of the effect of toluene concentration in the same manner of Au-Ami-SiO$_2$.

3.6.2   Equilibrium system

0.05 g of Au-Ami-SiO$_2$ was weighed and placed into a vial. Then 1.5 µL of liquid toluene was added in the vial and heated at 25, 75, 125, 175, 225 and 275 °C for 45 minutes. The gas products were characterized by the GC technique. The GC condition was shown in Table 3.3. The blank test and pure silica in each temperature was studied in the same manner of Au-Ami-SiO$_2$.

In equilibrium system, the maximum product of toluene oxidation condition was chosen to characterize by the GC-MS technique. The GC-MS condition was shown in Table 3.4.

Table 3.4 GC-MS condition for measurement of toluene vapor concentration.

Parameter	Operating condition
Column	VF-1 (30 m × 0.2 mm)
Injector temperature (°C)	250
Column temperature (°C)	50
Column flow (ml min^{-1})	1.0
Carrier gas	He
Mass analyzer	Ion trap
Injection volume (μL)	5

ศูนย์วิทยทรัพยากร
จุฬาลงกรณ์มหาวิทยาลัย

CHAPTER IV

RESULTS AND DISCUSSION

In this research, nanogold supported on amido-amidoxime functionalized silica (Au-Ami-SiO$_2$) has been prepared by a simple mixing of amido-amidoxime functionalized silica in the HAuCl$_4$ solution. The adsorption efficiency of nanogold on toluene vapor was studied and the catalytic performance of nanogold on oxidation of toluene in air was investigated. The results are shown below.

4.1 Characterization of materials

4.1.1 X-ray diffraction (XRD)

XRD is a crucial tool for phase analysis such that the characteristic structure of a crystalline material can be identified. In this work, XRD analysis was carried out for characterizing the structure of Ami-SiO$_2$ and Au-Ami-SiO$_2$.

XRD patterns were shown in Figure 4.1. The board peak appeared in Figure 4.1 (a) about 16-35° two theta was observed in the XRD pattern of Ami-SiO$_2$ corresponding to the amorphous silica characteristic and the XRD pattern of Au-Ami-SiO$_2$ (Figure 4.1 (b)) showed the characteristic peaks at 38, 44, 65 and 78° two theta indicating the 111, 200, 220 and 311 planes of a faced centered cubic lattice of gold nanoparticles, respectively [73]. The average gold crystalline size, determined by using the Scherrer equation on the most intense peak of (111) reflection, was 17.1 nm. Size of nanogold particle was 37 $\pm$ 6 nm which was measured by TEM technique [72].
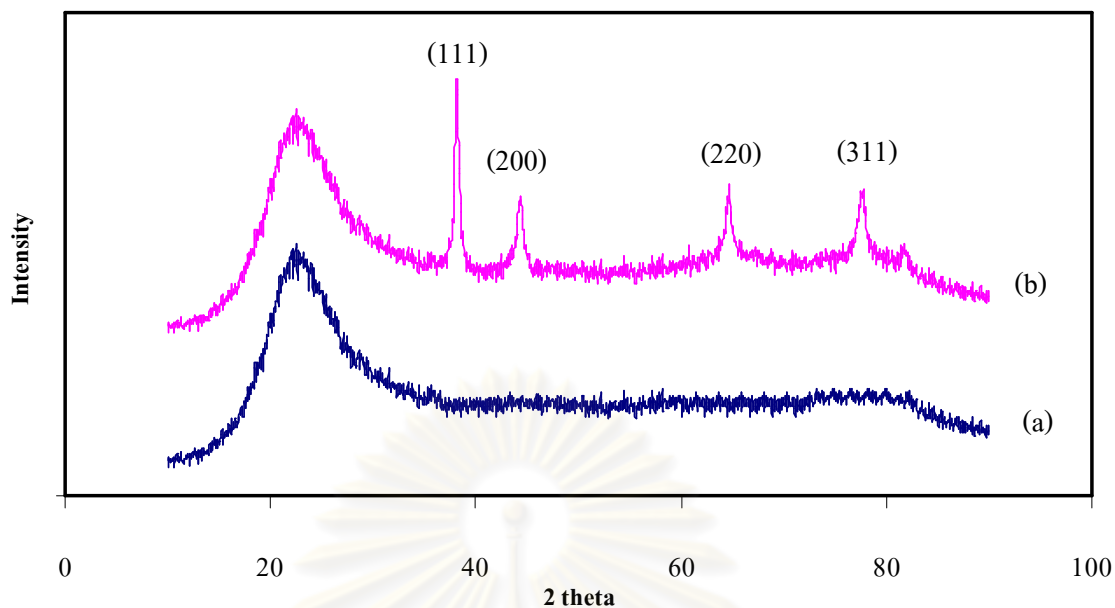
Figure 4.1 XRD patterns of (a) Ami-SiO$_2$ and (b) Au-Ami-SiO$_2$.

4.1.2 Surface area analyzer

The N$_2$ adsorption-desorption isotherm of SiO$_2$, Ami-SiO$_2$ and Au-Ami-SiO$_2$ are shown in Figure 4.2. All samples show a typical isotherm of type IV isotherm in the IUPAC classification. At low pressure (P/P$_0$ < 0.1), the rapid increase in nitrogen adsorption was found indicating a monolayer adsorption of N$_2$ on the surface. As the relative pressure increased (P/P$_0$ = 0.1 - 0.8), the adsorption increased and the hysteresis loop was obtained at P/P$_0$ = 0.5 - 0.8, which suggested the multilayer adsorption on the mesopores. At higher relative pressure (P/P$_0$ > 0.8), the plateau region was due to the fully pore filling followed by multilayer adsorption on the surface of the particles.
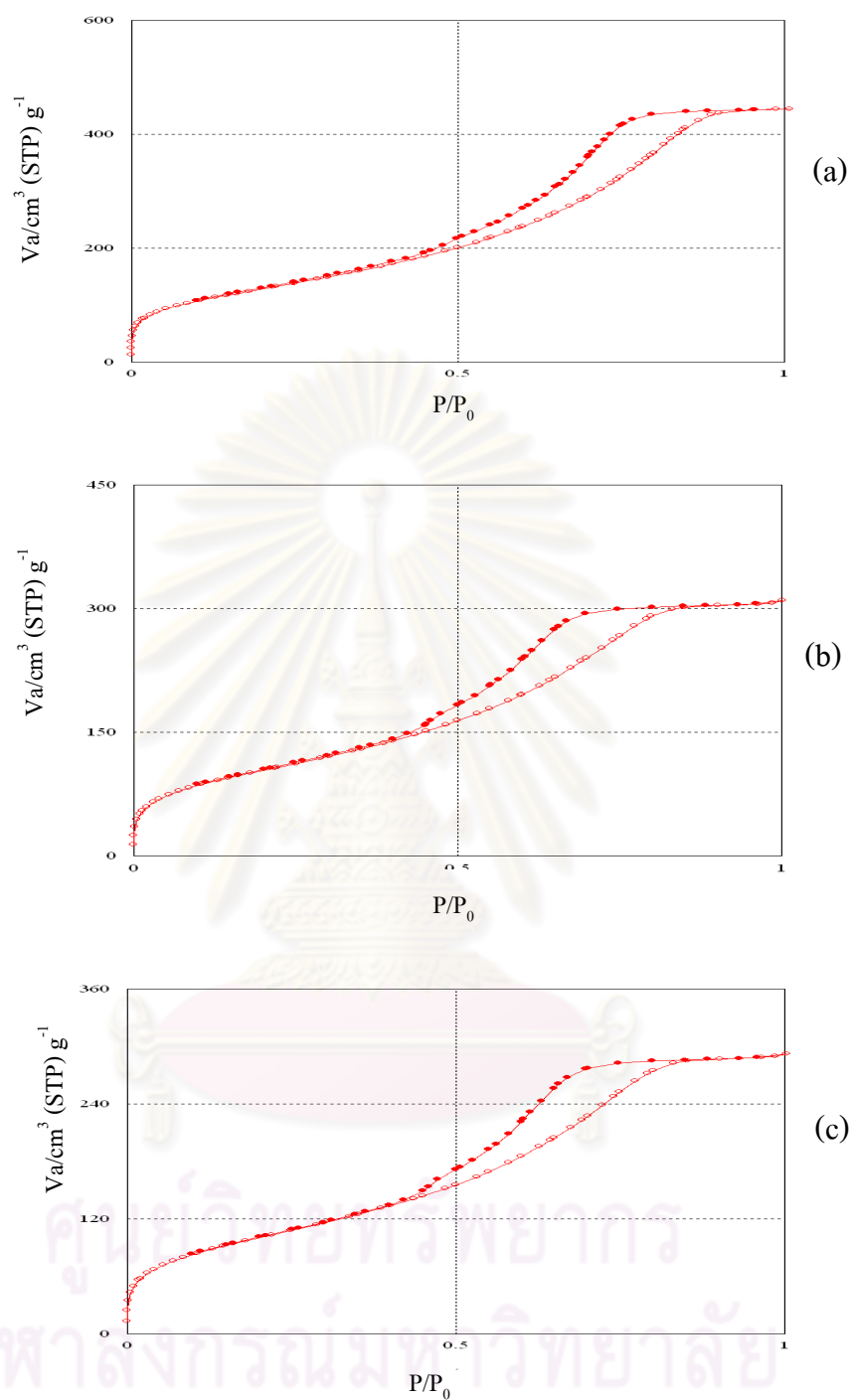
Figure 4.2 N$_2$ adsorption-desorption isotherm of (a) SiO$_2$, (b) Ami-SiO$_2$, and (c) Au-Ami-SiO$_2$.

The specific surface area of SiO_2, Ami-SiO_2 and Au-Ami-SiO_2 was determined by the Brunaunauer-Emmett-Teller method (BET). Pore volume and pore size distribution were calculated from the adsorption data by means of the Barrett, Joyner and Halenda (BJH) method. The results are shown in Table 4.1.

Table 4.1 Physicochemical properties of SiO_2, Ami-SiO_2 and Au-Ami-SiO_2 measured by the nitrogen adsorption-desorption isotherms

Sample	S_{BET}[a] $(m^2\ g^{-1})$	V_{avg}[b] $(cm^3\ g^{-1})$	D_{avg}[c] (nm)
SiO_2	463.9	0.671	3.28
Ami-SiO_2	376.6	0.462	3.71
Au-Ami-SiO_2	363.8	0.430	3.71

[a]Specific BET surface area

[b]Average BJH pore volume

[c]Average BJH pore diameter

The results show a significant decrease of surface area and pore volume in Au-Ami-SiO_2 compared to SiO_2 because pores may be covered and/or sealed by amidoxime groups and the gold particles. In addition, the amidoxime group has played role on the surface area and pore volume of silica support more than gold particles.

On the contrary, pore diameter of Ami-SiO_2 was larger than that of SiO_2. This may be pore wall of SiO_2 and was explained that partially destroyed in the preparation step of Ami-SiO_2. However, there are no difference in pore diameters of Ami-SiO_2 and Au-Ami-SiO_2, suggesting Au has not affected on the pore structure.

The results from XRD and surface area analyzer confirm the successful preparation of nanogold supported amido-amidoxime functionalized silica (Au-Ami-

SiO$_2$). The Au-Ami-SiO$_2$ was further used in the adsorption and oxidation of toluene vapour.

4.2 Adsorption study

The nanogold supported on amido-amidoxime functionalized silica (Au-Ami-SiO$_2$) was used for the adsorption study of toluene vapour using a fixed bed system. The effect of various parameters such as contact time, flow rate, and adsorbent dose were investigated in order to obtain an optimum condition for toluene oxidation.

The toluene adsorption efficiency is presented in term of adsorption capacity (q), calculated according to equation A-1.

4.2.1 Effect of contact time and flow rate

The adsorption of gas (adsorbate) on solid (adsorbent) can occur according to the following steps. In the first step, the contaminant diffuses from the major body of the air stream to the external surface of the adsorbent particle. In the second step, the contaminant molecule migrates from the relatively small area of the external surface to the pores within each adsorbent particle. The bulk of adsorption occurs in these pores because the majority of available surface area in there. In the third step, the contaminant molecule adheres to the surface in the pore [54]. Thus, adsorption phenomena are mainly controlled by the external and interparticle diffusion which their kinetics of mass transport are depended on the time. In this experiment, the effects of contact time and flow rate were investigated to obtain the equilibrium time for the adsorption process.

The experiment was carried out by fixing volume of toluene vapour, which could be calculated by equation 4.1.

$$V = F \times t \qquad\qquad (4.1)$$

where; V = volume of toluene vapour, F = flow rate of stream and t = contact time

Since the volume of toluene vapour was constant, the flow rate of the reaction was varied as follows; 40, 60 and 80 mL min^{-1}. Therefore, the gas flow time would be 15, 10, and 7.5 minutes, respectively.

Figure 4.3 and Table 4.2 show that the adsorption capacity increases with increasing contact time until the maximum adsorption capacity (q_{max}) is reached (maximum adsorption capacity, q_{max}) afterward the adsorption capacity slightly decreased. This is because after the q_{max} point, the availability of active sites possibly decreased. And when the flow rate increased, the q_{max} obviously decreased because in higher flow rate systems, the amount of toluene passed through the fixed bed of adsorbent increased and t_{max} was thus decreased. The efficiency of adsorbent was decreased with increasing the flow rate probably due to the fact that the contact time between toluene molecules and adsorbent surface was shorter. In this work, the flow rate of 40 mL min^{-1} was chosen for further experiments.

The experiment procedure of the last two points in every experiment presented in Figure 4.3 was slightly different from the others, the collection of gas phase by Tedlar® bag was modified that two and three bags were used instead of one in the fourth and fifth adsorption experiments, respectively due to the limit of bag volume and toluene content in each bag was analyzed by GC technique. The adsorption capacity was calculated based on the difference between the peak area of toluene without adsorbent (A_0) and that of toluene with adsorbent (A_f) and the two or three stages of toluene adsorption capacity; resulting from the toluene content in second or third Tedlar® bags were assembled. From GC data of the second and/or third Tedlar® bag, A_f was higher than A_0, this observation revealed that toluene content in the outlet of the adsorbent bed decreased. The desorption of toluene previously adsorbed onto

Au-Ami-SiO$_2$ might occur. This phenomena might be described by the fact that, after the q$_{max}$ point, there was no liquid toluene in the saturator (toluene was bubbled until dryness) resulting that the toluene vapour concentration in gas phase diminished and became zero (pure argon). When pure argon passed through the adsorbent, the adsorption equilibrium expressed in Equation 4.2 was disturbed. According to *Le Chatelier's* principle, the equilibrium was driven to the right, resulting in desorption of toluene from the sorbent surface into the gas phase. Thus, A_f was higher than A_0.

$$(\text{Toluene})_{\text{adsorbent}} \rightleftharpoons (\text{Toluene})_{\text{gas phase}} \qquad (4.2)$$
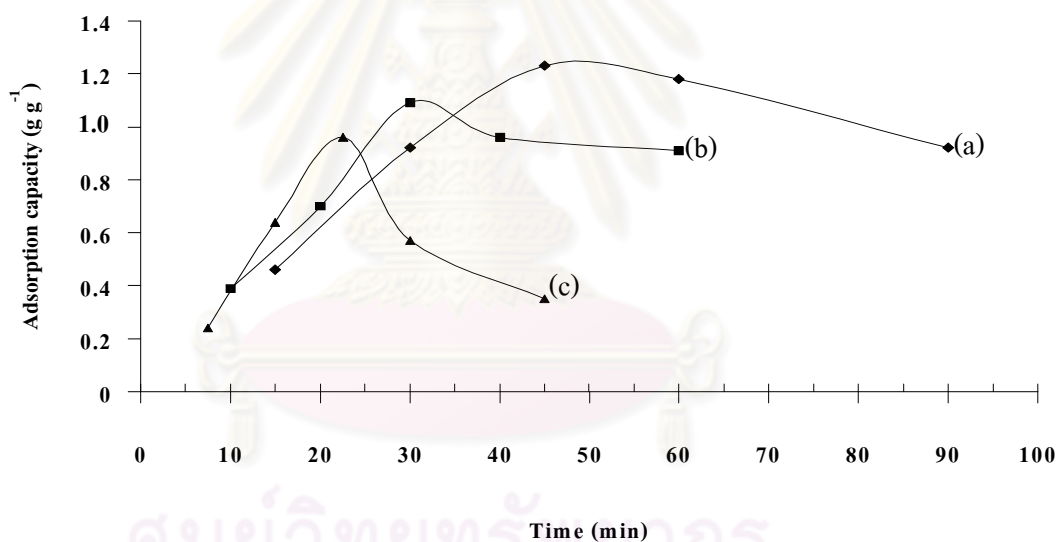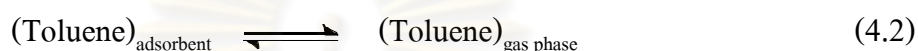
Figure 4.3 Adsorption of toluene on Au-Ami-SiO$_2$, flow rate:(a) 40 mL min^{-1} (b) 60 mL min^{-1} and (c) 80 mL min^{-1}, toluene adsorption condition was 0.1 g of Au-Ami-SiO$_2$ at 25 $\pm$1°C.

Table 4.2 Effect of contact time and flow rate on adsorption capacity of toluene vapour onto Au-Ami-SiO$_2$

Ar flow rate (mL min^{-1})	Contact time (minute)	Initial toluene concentration (mg m^{-3})[a]	Adsorption capacity (g g^{-1})[b]
	15	419.78 ± 34.97	0.46 ± 0.00
	30	491.00 ± 57.65	0.92 ± 0.01
40	45	591.43 ± 89.25	1.23 ± 0.01
	60	480.40 ± 74.83	1.18 ± 0.02
	90	524.19 ± 23.57	0.92 ± 0.02
	10	419.78 ± 34.97	0.39 ± 0.01
	20	491.00 ± 57.65	0.70 ± 0.01
60	30	591.43 ± 89.25	1.09 ± 0.01
	40	480.40 ± 74.83	0.96 ± 0.02
	60	524.19 ± 23.57	0.90 ± 0.02
	7.5	419.78 ± 34.97	0.24 ± 0.01
	15	491.00 ± 57.65	0.64 ± 0.01
80	22.5	591.43 ± 89.25	0.96 ± 0.02
	30	480.40 ± 74.83	0.57 ± 0.01
	45	524.19 ± 23.57	0.35 ± 0.01

[a]The concentration of toluene vapour was fixed 0.4 mL liquid toluene and varied volume (flow rate x contact time)

[b]Mean (range), n = 2.

4.2.2 Effect of adsorbent dose

The effect of adsorbent dose on toluene vapour adsorption was studied in order to observe the adsorption behavior of Au-Ami-SiO$_2$ by varying the amount of the adsorbent in the range of 0.05 to 0.2 g. Furthermore, for each adsorbent dose at 40 mL min^{-1} flow rate, the contact time was also varied in the range of 0 to 60 min.
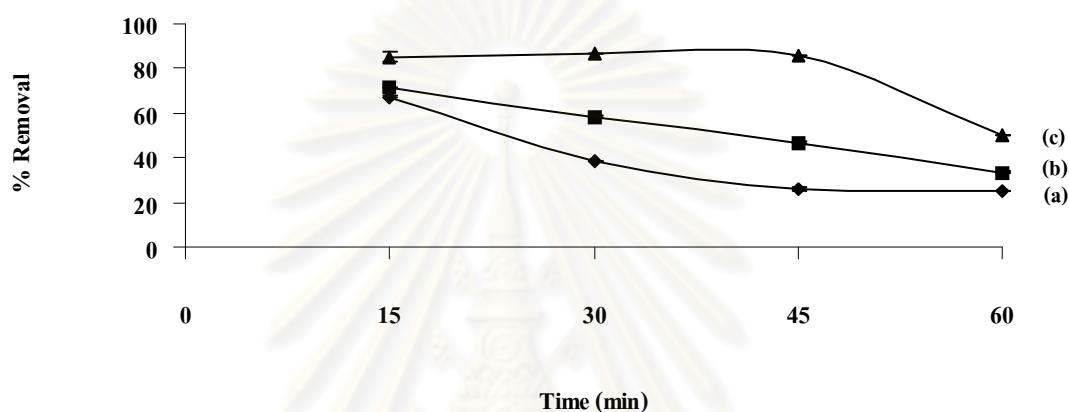
Figure 4.4 Effect of adsorbent dose on toluene removal:(a) 0.05 g (b) 0.1 g and (c) 0.2 g, toluene adsorption condition was at flow rate 40 mL min^{-1} of Au-Ami-SiO$_2$ at 25 $\pm 1^{\circ}$C.

Figure 4.4 demonstrated the percentage removal of toluene on Au-Ami-SiO$_2$ at different adsorbent dose. The percentage removal could be calculated from equation 4.3 (Section 4.3). The result shows that the percentage removal increased when increasing adsorbent dose. It could be explained that active sites increase at higher adsorbent dose. However, the percentage removal decreased when increasing contact time because toluene was bubbled until dryness and pure argon gas passed through the sorbent, then the desorption occurred as explained in the previous section.

The adsorption capacity at different adsorbent doses was presented Table 4.3. It was observed that the higher the adsorbent amount, the lower the adsorption capacity. Actually, the adsorption capacity was expressed as amount of toluene adsorbed per

unit mass of adsorbent. In our experimental condition, the adsorbent dose of 0.05 g showed the highest adsorbality. Therefore, the adsorbent dose of 0.05 g was chosen for further study.

Table 4.3 Effect of adsorbent dose on adsorption capacity of toluene vapour onto Au-Ami-SiO$_2$

Adsorbent dose (g)	Contact time (min)	Initial toluene concentration (mg m^{-3})[a]	Adsorption capacity (g g^{-1})[b]
0.05	15	401.01 ± 1.77	0.85 ± 0.01
	30	498.39 ± 0.56	1.21 ± 0.00
	45	551.24 ± 1.86	1.36 ± 0.04
	60	498.39 ± 0.56	0.37 ± 0.00
0.1	15	401.01 ± 1.77	0.46 ± 0.00
	30	498.39 ± 0.56	0.92 ± 0.01
	45	551.24 ± 1.86	1.23 ± 0.01
	60	498.39 ± 0.56	1.18 ± 0.02
0.2	15	401.01 ± 1.77	0.27 ± 0.01
	30	498.39 ± 0.56	0.68 ± 0.00
	45	551.24 ± 1.86	1.12 ± 0.00
	60	498.39 ± 0.56	0.89 ± 0.01

[a]The amount of toluene was fixed at 0.4 mL of liquid toluene and Ar flow rate of 40 mL min^{-1}

[b]Mean (range), n = 2.

In conclusion, the appropriate condition for the adsorption of toluene vapour by Au-Ami-SiO$_2$ was 45 min contact time, 40 mL min^{-1} flow rate and 0.05 g Au-Ami-SiO$_2$. The maximum adsorption capacity was 1.36 g g^{-1}. This condition was chosen for further study.

When comparing the adsorption capacity of other adsorbents reported in Table 4.4. The adsorption capacity of prepared adsorbent in this work was higher than previous researches. Therefore, Au-Ami-SiO$_2$ was obviously a better adsorbent for toluene vapour.

Table 4.4 Comparison of maximum adsorption capacity of various sorbents

Solid support	q_{max} (mol g^{-1})	Ref.
Silica	0.0013	[67]
Mesoporous silicalite-1 nanospheres (Zeolite)	0.0049	[68]
Activated carbon	0.0059	[69]
MCM-41	0.0066	[70]
Silica (TMOS)[a]	0.0119	[7]
Au-Ami-SiO$_2$	0.0148	This work

[a]Tetramethoxysilane was used for silica synthesis.

4.3   Catalytic oxidation

The Au-Ami-SiO$_2$ was used in catalytic oxidation study of toluene vapour in the continuous system. The effects of reaction temperature and toluene concentration were investigated.

In this work, the activity of catalyst was reported in term of percentage removal calculated according to equation 4.3 by using peak areas obtained from GC analysis,

$$\text{Removal (\%)} = \frac{A_o - A_f}{A_o} \, x \, 100 \qquad\qquad (4.3)$$

Where A_0 = Peak area of toluene at the outlet of the reactor without catalyst

A_f = Peak area of toluene at the outlet of the reactor with catalyst

4.3.1 Effect of temperature

The effect of temperature is one of parameters that have strong influence in the catalytic oxidation of volatile organic compounds. The percentage removal from catalytic oxidation of toluene over Au-Ami-SiO$_2$ and SiO$_2$ were investigated as a function of reaction temperature. The temperature reaction was 25, 75, 125 and 175 $^\circ$C. The reaction conditions were fixed at reaction time of 45 minutes, air flow rate of 40 mL min^{-1} and 0.05 g of catalyst dose. The results are shown in Figure 4.5 and Table 4.5.
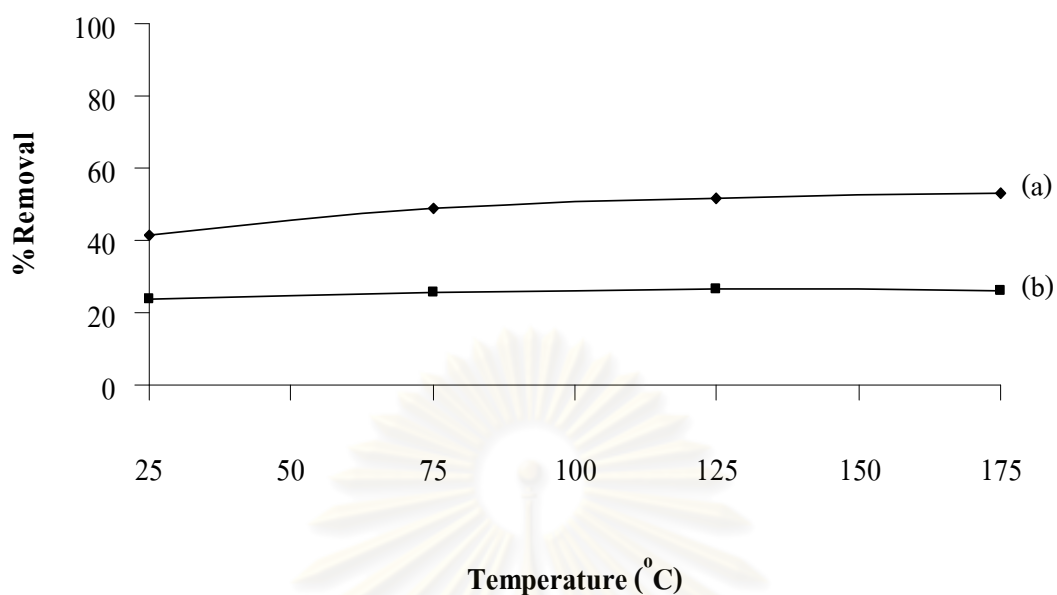
Figure 4.5 Catalytic oxidation of toluene on: (a) Au-Ami-SiO$_2$ and (b) SiO$_2$, reaction condition was at reaction time 45 min, air flow rate 40 mL min^{-1} and 0.05 g of catalyst at 25 – 175 $\pm$ 3 °C.

Figure 4.5 demonstrated the percentage removal of toluene over Au-Ami-SiO$_2$ and SiO$_2$ at different temperatures. When the temperature increased from 25 to 175 °C, the percentage removal increased continuously until it reached a maximum percentage removal at 53.06 $\pm$ 0.04 % in Au-Ami-SiO$_2$ at 175 °C, the toluene and unknown peaks appeared in Figure A-3 by GC technique. The unknown peak was identified by GC-MS. MS spectrum of the final product showed m/z = 44 and 91, which are the molecular mass of CO$_2$ and toluene, respectively shown in Figure A-5. So the oxidation reaction temperature appeared at 175 °C in Au-Ami-SiO$_2$, which was confirmed by GC and GC-MS technique. At reaction temperature lower 175 °C disappeared CO$_2$ peak so percentage removal related to only influence of adsorption in this temperature range. The increase in percentage removal corresponds to the increase in the temperature.

Comparing between Au-Ami-SiO$_2$ and SiO$_2$ at the same reaction temperature, it was found that Au-Ami-SiO$_2$ showed higher toluene vapour removal than that of pure SiO$_2$ because SiO$_2$ appeared only physisorption but Au-Ami-SiO$_2$ able to chemisorption and physisorption with toluene vapour. So, the reaction temperature of 175 °C was selected for further studies.

Table 4.5 Catalytic oxidation of toluene over SiO$_2$ and Au-Ami-SiO$_2$ at various reaction temperatures

Reaction temperature (°C)	Sample	%Removal
25	SiO$_2$	23.69 $\pm$ 0.36
	Au-Ami-SiO$_2$	41.27 $\pm$ 0.45
75	SiO$_2$	25.70 $\pm$ 0.30
	Au-Ami-SiO$_2$	49.05 $\pm$ 0.39
125	SiO$_2$	26.36 $\pm$ 0.64
	Au-Ami-SiO$_2$	51.67 $\pm$ 0.51
175	SiO$_2$	26.14 $\pm$ 0.04
	Au-Ami-SiO$_2$	53.06 $\pm$ 0.04

Reaction condition: Air flow of 40 mL min^{-1}, 45 min reaction time and 0.05 g catalyst dose .

When comparing the 50 percent removal of gold particle on other solid supports reported in the literatures (Table 4.6), the prepared catalyst in this work was active at the temperature lower than other previous researches. In Table 4.6, the temperature with 50 percent removal ($T_{50\%}$) was reported. The $T_{50\%}$ of our experiment was determined from Figure 4.5 and Table 4.5. Thereby, Au-Ami-SiO$_2$ is a good candidate for catalytic oxidation of toluene.

Table 4.6 The 50 percentage removal of gold particle on other solid supports for toluene removal in the continuous system

Sample	$T_{50\%}$ toluene removal (°C)[a]	Ref.
Au/Fe$_2$O$_3$	290	[13]
Au/CeO$_2$	271	[5]
Au/TiO$_2$	217	[15]
Au-Pd/TiO$_2$	223	[15]
Au-Ami-SiO$_2$	125	This work

[a]$T_{50\%}$ = temperature was 50 percentage removal of toluene.

4.3.2 Effect of concentration of toluene

The effect of the toluene concentration in the oxidation of toluene over Au-Ami-SiO$_2$ was investigated. The toluene concentration was 190, 334, 511 and 685 mg m^{-3}. In this range (100-1000 mg m^{-3}) effect to human health [2]. The results in Table 4.7 and Figure 4.6 show the percentage removal of toluene over Au-Ami-SiO$_2$ and SiO$_2$ at different initial concentrations. It was seen that the percentage removal increased abruptly from around 0 – 190 mg m^{-3} when the initial concentration increased (from 190 to 685 mg m^{-3}), percentage removal increased continuously until it reached a maximum percentage removal at 53.06 % by 685 mg m^{-3}. The increase in percentage removal corresponds to increase in the initial concentration.

Comparing the percentage removal between Au-Ami-SiO$_2$ and SiO$_2$ at the same initial concentration, that of Au-Ami-SiO$_2$ was higher than that of pure SiO$_2$. This reason was described in Section 4.3.1. So, the 685 mg m^{-3} initial concentration at 175°C was selected for further studies.
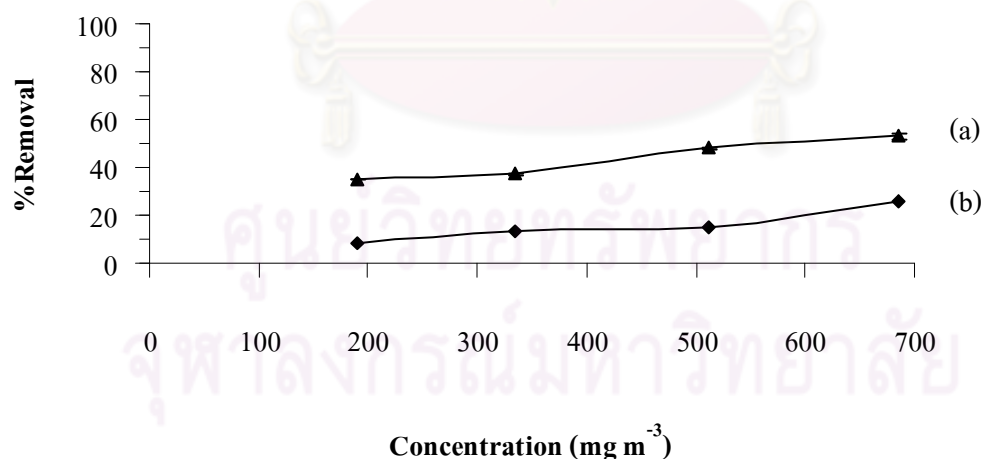
Figure 4.6 Catalytic oxidation of toluene on: (a) Au-Ami-SiO$_2$ and (b) SiO$_2$ at various the toluene concentrations, reaction condition was at reaction time 45 min, air flow rate 40 mL min^{-1} and 0.05 g of catalyst at 175 °C.

Table 4.7 Catalytic oxidation of toluene over SiO_2 and Au-Ami-SiO_2 at various toluene concentrations

Toluene concentration ($mg\ m^{-3}$)	sample	%Removal
190	SiO_2	8.15 ± 0.67
	Au-Ami-SiO_2	35.09 ± 0.48
334	SiO_2	13.51 ± 0.48
	Au-Ami-SiO_2	37.37 ± 045
511	SiO_2	15.17 ± 1.03
	Au-Ami-SiO_2	48.11 ± 0.35
685	SiO_2	26.14 ± 0.04
	Au-Ami-SiO_2	53.06 ± 0.04

Reaction condition: Air flow of 40 mL min^{-1}, the reaction time 45 min and catalyst dose of 0.05 g.

4.3   Equilibrium system

The Au-Ami-SiO$_2$ was used in catalytic oxidation study of toluene vapour in the equilibrium system. The effect of reaction temperature was investigated.

The effect of temperature in the oxidation of toluene over Au-Ami-SiO$_2$ and SiO$_2$ were investigated. The temperature reaction was 25, 75, 125, 175, 225 and 275 $^{\circ}$C. The concentration of toluene was around 685 mg m^{-3} with 45 min reaction time and 0.05 g Au-Ami-SiO$_2$. The results are collected in Figure 4.7 and Table 4.8.

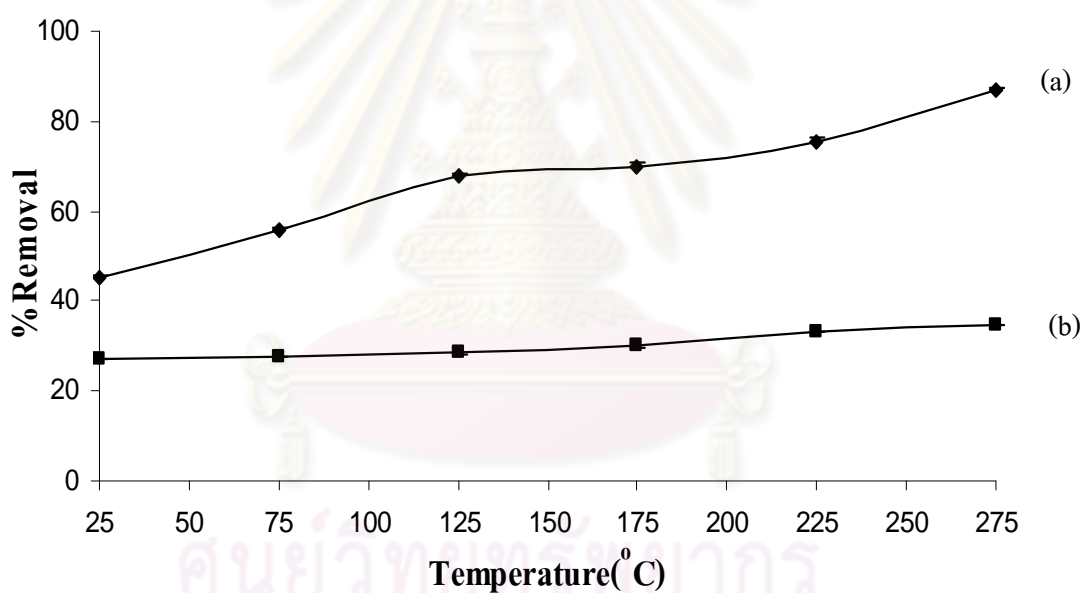**Figure 4.7** Catalytic oxidation of toluene over (a) Au-Ami-SiO$_2$ and (b) SiO$_2$ at various reaction temperatures in the equilibrium system.

From Figure 4.7 and Table 4.8, it can be seen that the percentage removal of toluene over Au-Ami-SiO$_2$ at different temperatures slightly increased in two steps; in

the first step , the percentage removal in the range of 25 – 175 °C, it was the same trend in Section 4.2.1 because toluene vapour was adsorbed to equilibrium point. In the second step (175 – 275 °C), the percentage removal clearly increased because nanogolds probably enhance the combustion of toluene. So toluene was oxidized in that temperature range. The CO_2 appeared at 175 °C, the increase in CO_2 corresponds to increase in reaction temperature until it reached a maximum percentage removal at 87.11 $\pm$ 0.15 %, at 275 °C.

For the SiO_2 system, percentage removal was not different in every temperature reaction when it was compared with the continuous system. So the result indicated that SiO_2 did not facilitate the oxidation reaction of toluene.

Comparing the percentage removal between continuous system and equilibrium system at 175 °C (53.06 $\pm$ 0.04 % and 70.09 $\pm$ 0.86 %), respectively, the percentage removal of equilibrium system was higher than that of continuous system. This may be due to the effect of contact time of toluene on catalyst surface. The contact time of toluene molecules on Au-Ami-SiO_2 in the equilibrium system was longer than that in the continuous system.

Table 4.8 Catalytic oxidation of toluene over SiO_2 and Au-Ami-SiO_2 catalyst at various the reaction temperatures in equilibrium system

Reaction temperature (°C)	Sample	%Removal
25	SiO_2	27.26 ± 0.17
	Au-Ami-SiO_2	45.36 ± 0.16
75	SiO_2	27.60 ± 0.17
	Au-Ami-SiO_2	55.90 ± 0.29
125	SiO_2	28.53 ± 0.41
	Au-Ami-SiO_2	68.02 ± 0.18
175	SiO_2	29.98 ± 0.15
	Au-Ami-SiO_2	70.09 ± 0.86
225	SiO_2	33.06 ± 0.04
	Au-Ami-SiO_2	75.49 ± 0.86
275	SiO_2	34.88 ± 0.25
	Au-Ami-SiO_2	87.11 ± 0.15

Reaction condition: the reaction time 45 min, catalyst dose of 0.05 g and 685 mg m^{-3} initial toluene concentration.

CAPTER V

CONCLUSION

Nanogold supported on amido-amidoxime functionalized silica (Au-Ami-SiO_2) was prepared by a simple mixing of amido-amidoxime functionalized silica (Ami-SiO_2) in the $HAuCl_4$ solution. Then, Au-Ami-SiO_2 was characterized by X-ray diffraction (XRD) technique and surface area analyzer. The results from all techniques confirmed the successful preparation of Au-Ami-SiO_2.

In the adsorption study, Au-Ami-SiO_2 was applied for the removal of toluene vapour using a fixed bed system. The effects of contact time, flow rate and adsorbent dose were investigated. The appropriate condition for the adsorption of toluene vapour by Au-Ami-SiO_2 was 45 min contact time, 40 mL min^{-1} flow rate and 0.05 g Au-Ami-SiO_2 at ambient temperature. The maximum adsorption capacity was 1.36 g g^{-1}.

Moreover, the catalytic property of Au-Ami-SiO_2 was investigated for toluene vapour oxidation at the appropriate condition under air atmosphere. The effects of reaction temperature and toluene concentration were investigated in two systems: the first was coctinuous system and the second was batch system. In the coctinuous system, the reaction temperature and toluene concentration were studied in range of 25 – 175 °C and 190 – 685 mg m^{-3}, respectively. From the results, the highest % removal was 53.06 ± 0.04 % at 685 mg m^{-3}, at 175 °C. The batch system was studied in range of 25 – 275 °C with fixed toluene concentration at 685 mg m^{-3}, the highest % removal was 87.11 ± 0.15 % at 275 °C. The oxidative product appeared at 175 °C and when the reaction temperature increased the oxidative product increased. The product was identifed by GC-MS and CO_2 was found as the main product.

The comparison in % toluene removal between Au-Ami-SiO$_2$ with SiO$_2$ showed that at temperature above 175 °C, Au-Ami-SiO$_2$ can enhance the oxidative reaction of toluene.

Suggestions for Future Work

The reuse of adsorbent and the higher reaction temperature in the continuous system should be investigated. The oxidative product should be examined quantitatively.

REFERENCES

[1] Removal of Volatile Organic Compounds by Biological Approach (Phase 1-2) [Online]. (n.d.). Available from: http://www.kmutt.ac.th/rippc/volati.htm [2009, October 12].

[2] Toluene [Online]. U. S. EPA. Available from: http://www.epa.gov/ttn/atw/hlthef/toluene.html [2009, October 18].

[3] Faisal, I. K.; and Aloke, Kr. G. Removal of volatile organic compounds from polluted air. Journal of Loss Prevention in the Process Industries 13 (2000): 527-545.

[4] Carpentier, J.; Lamonier, J. F.; Siffert, S.; Zhilinskaya, E. A.; and Aboukais, A. Characterisation of Mg/Al hydrotalcite with interlayer palladium complex for catalytic oxidation of toluene. Applied Catalysis A: General 234 (2002): 91-101.

[5] Scire, S.; Minico, S.; Crisafulli, C.; Satriano, C.; and Pistone, A. Catalytic combustion of volatile organic compounds on gold/cerium oxide catalysts. Applied Catalysis B: Environmental 40 (2003): 43-49.

[6] Lin, E.; Lu, Y.; and Zeng, H. Extraction of gold from Au(III) ion containing solution by a reactive fiber. Journal of Applied Polymer Science 49 (1993): 1635-1638.

[7] Standeker, S.; Novak, Z.; and Knez, Z. Removal of BTEX vapours from waste gas streams using silica aerogels of different hydrophobicity. Journal of Hazardous Materials 165 (2009): 1114-1118.

[8] Wang, C. M.; Chang, K. S.; and Chung, T. W. Adsorption equilibria of aromatic compounds on activated carbon, Silica Gel, and 13X zeolite. Journal of Chemical and Engineering Data 49 (2004): 527-531.

[9] Buamra, W. S.; Baker, C. G. J.; Elkilani, A. S.; Alkandari, A. A.; and Al-Mansour. A. A. A. Adsorption of toluene and 1,1,1-trichloroethane on selected adsorbents under a range of ambient conditions. Adsorption 15 (2009): 461-475.

[10] Centeno, M. A.; Paulis, M.; Montes, M.; and Odriozola, J. A. Catalytic combustion of volatile organic compounds on $Au/CeO_2/Al_2O_3$ and Au/Al_2O_3 catalysts. Applied Catalysis A: General 234 (2002): 65-78.

[11] Minico, S.; Scier, S.; Crisafulli, C.; Maggiore, R.; and Galvagno, S. Catalytic combustion of volatile organic compounds on gold/iron oxide catalysts. Applied Catalysis B: Environmental 28 (2000): 245-251.

[12] Minico, S.; Scier, S.; Crisafulli, C.; and Galvagno, S. Influence of catalyst pretreatment on volatile organic compounds oxidation over gold/iron oxide. Applied Catalysis B: Environmental 34 (2001): 277-285.

[13] Scier, S.; Minico, S.; Crisafulli, C.; and Galvagno, S. Catalytic combustion of volatile organic compounds over group IB metal catalyst on Fe_2O_3. Catalysis Communications 2 (2001): 229-232.

[14] Gluhoi, A. C.; Bogdanchikova, N.; Nieuwenhuys, B. E. Journal of Catalysis 229 (2005): 154-162.

[15] Hosseini, M.; Siffert, S.; Tidahy, H. L.; Cousin, R.; Lamonier, J. -F.; Aboukais, A.; Vantomme, A.; Roussel, M.; and Su, B. –L. Promotional effect of gold added to palladium supported on a new mesoporous TiO_2 for total oxidation of volatile organic compounds. Catalysis Today 122 (2007): 391-396.

[16] Ivanova, S.; Petit, C.; and Pitchon, V. A new preparation method for the formation of gold nanoparticles on oxide support. Applied Catalysis A 267 (2004): 191-201.

[17] Chen, Y.; Qiu, J.; Wang, X.; and Xiu, J. Preparation and application of highly dispersed gold nanoparticles supported on silica for catalytic hydrogenation of aromatic nitro compounds. Journal of Catalysis 242 (2006): 227-230.

[18] Properties of gold [online]. Utilise Gold. Avi0able from: http://www. utilisegold. com/uses_applications/properties_of_gold/ [2009, October 18].

[19] Puddephatt, R. J.; and Vittal, J. J. Gold: inorganic & coordinate chemistry. Chichester UK: John Wiley & Sons, (1994).

[20] Puddephatt, R. J. The chemistry of gold. New York, Elsevier Scientific Publishing Company, (1978).

[21] Bond, G. C.; and Thompson, D. T. Catalysis by gold. Catalysis Reviews-Science and Engineering 41 (1999): 319-388.

[22] Read, H. H. Rutley's elements of mineralogy. 26[th]ed. London, Thomas Murby & Co., (1970).

[23] Cleveland, C. L.; Landman, U.; Schaaf, T. G.; and Shafigullin, M. N. Structural evolution of smaller gold nanocrystals: the truncated decahedral motif. Physical Review Letters 79 (1997): 1873-1876.

[24] Cortie, M.B.; and Lingen E. V. Catalytic gold nano-particles. Materials Forum 26 (2002): 1-14.

[25] Haruta, M. Size- and support-dependency in the catalysis of gold. Catalysis Today 36 (1997): 153-166.

[26] Haruta, M.; Tsubota, S.; Kobayashi, T.; Kageyama, H.; Genetand, M. J.; and Delmon, B. Low-temperature oxidation of CO over gold supported on TiO_2, α-Fe_2O_3, and Co_3O_4. Journal of Catalysis 144 (1993): 175-192.

[27] Daniel, M. C.; and Astruc, D. Gold nanoparticlee: assembly, supramolecular chemistry, quantum-size-related properties, and applications toward biology, catalysis, and nanotechnology. Chemical Reviews 104 (2004): 293-346.

[28] Pal, A.; Pal, T.; Stokes, D. L.; and Vo-Dinh, T. Photochemically prepared gold nanoparticles: a substate for surface Current Science 84 (2003): 1342-1345.

[29] Patungwasa, W.; and Hodak, J. H. pH tunable morphology of the gold nanoparticles produced by citrate reduction. Materials Chemistry and Physics 108 (2008): 45-54.

[30] Mandal, S.; et al. Synthesis of a stable gold hydrosol by the reduction of chloroaurate ions by the amino acid, aspartic acid. Journal of Chemical Sciences 114 (2002): 513-520.

[31] Stremsdoerfer, G.; et al. Autocatalytic deposition of gold and palladium onto n-GaAs in acidic media. Journal of the Electrochemical Society 135 (1988): 2881-2886.

[32] Duff, D.G.; Baiker, A.; and Edwards, P. P. A new hydrosol of gold clusters. 1. Formation and particle size variation. Langmuir 9 (1993): 2301-2309.

[33] Patil, V.; Malvankar, R. B.; and Sastry, M. Role of particle size in individual and competitive diffusion of carboxylic acid derivatized colloidal gold particles in thermally evaporated fatty amine films. Langmuir 15 (1999): 8197-8206.

[34] Tsunoyama, H.; Sakurai, H.; Ichikuni, N.; Negishi, Y.; and Tsukuda, T. Colloidal gold nanoparticles as catalyst for carbon-carbon bond formation: application to aerobic homocoupling of phenylboronic acid in water. Langmuir 20 (2004): 11293-11296.

[35] Turkevitch, J.; Stevenson, P. C.; and Hillier, J. Nucleation and growth process in the synthesis of colloidal gold. Discussions of the Faraday Society 11 (1951): 55-75.

[36] Colloidal gold [Online]. Wikipedia, the free encyclopedia. Avialable from: http://en.wikipedia.org/wiki/Colloidal_gold [2009, October 18].

[37] Yonezawa, T.; and Kunitake, T. Practical preparation of anionic mercapto ligand stabilized gold nanoparticles and their immobilization. Colloids Surface A: Physicochemical and Engineering Aspects 149 (1999): 193-199.

[38] Brust, M.; et al. Synthesis of thiol-derivatised gold nanoparticles in a two-phase liquid- liquid system. Journal of the Chemical Society, Chemical Communications (1994): 801-802.

[39] Brust, M.; et al. Synthesis and reactions of functionalized gold nanoparticles. Journal of the Chemical Society, Chemical Communications (1995): 1655-1656.

[40] Moriguchi, I.; et al. Synthesis of gold particles in organized molecular assembly films. Colloids Surface A: Physicochemical and Engineering Aspects 126 (1997): 159-166.

[41] Jana, N. R.; Gearheart, L.; and Murphy, C. J. Evidence for seed-mediated nucleation in the chemical reduction of gold salts to gold nanoparticles. Chemistry of Materials 13 (2001): 2313-2322.

[42] Sau, T. K.; Pal, A.; Jana, N.R.; Wang, Z. L.; and Pal, T. Size controlled synthesis of gold nanoparticles using photochemically prepared seed particles. Journal of Nanoparticle Research 3 (2001): 257-261.

[43] Meltzer, S.; Resch, R.; Koel, B. E.; Thompson, M. E.; Madhukar, A.; Requicha, A. A. G.; and Will, P. Fabrication of nanostructures by hydroxylamine seeding of gold nanoparticles templates. Langmuir 17 (2001): 1713-1718.

[44] Carrot, G.; Valmalette, J.; Plummer, C. J. G.; Scholz, S. M.; Dutta, J.; Hofmann, H.; and Hilborn, J. G. Gold nanoparticle synthesis in graft copolymer micelles. Colloid and Polymer Science 276 (1998): 853-859.

[45] Gold [online]. Gold Bull. Aviable from: http://www.goldbulletin.org [2009, October 18].

[46] Bond, G. C; Louis, C.; and Thompson, D. T. Catalysis by gold. London: Imperial College Press., (2006).

[47] Zosel, J.; Westphal, D.; Jakobs, S.; Muller, R.; and Guth, U. Au-oxide composites as HC-sensitive electrode material for mixed potential gas sensors. Solid State Ionics 152 (2002): 525-529.

[48] Schmidt-Zhang, P.; and Guth, U. A planar thick film sensor for hydrocarbon monitoring in exhaust gases. Sensors and Actuators B-Chemical 99 (2004): 258-263.

[49] Corti, C. W.; Holliday, R. J.; and Thomson, D. T. Developing new industrial applications for gold: gold nanotechnology. USA: World Gold Council., (2002).

[50] Corti, C. W.; and Holliday, R. J. Gold science and applications. USA: Taylor & Francis Group., (2010).

[51] Volatile Organic Compounds [online]. Encyclopedia of the Atmospheric Environment. Aviable from: http://www.ace.mmu.ac.uk/eae/air_quality/ Older/VOCs.html [2009, October 18].

[52] Definition for Volatile Organic Compounds (VOCs) [online]. (n.d.) Aviable from: http://www2.unitar.org/cwm/publications/clb/prtr/pdf/cat5/voc.pdf [2009, October 18].

[53] Bloemen, H. J. Th.; and Burn, J. Chemistry and analysis of volatile organic compounds in the environment. 1sted. UK: Blackie Academic & Professional, Inc., (1993).

[54] Volatile Organic Compounds [online]. Wikia Green. Aviable from: http://green.wikia.com/wiki/Volatile_Organic_Compound_(VOC) [2009, October 18].

[55] Indoor Air Pollution [online]. The Clean Air Coach. Aviable from: http://www.the-air-purifier-for-you.com/indoor-air-pollution-chemicals.html [2009, October 18].

[56] Chronic Toxicity Summary Toluene [online]. U. S. EPA. Aviable from: http://oehha.ca.gov/air/ chronic_ rels/ pdf/108883.pdf [2009, October 18].

[57] Greenberg, M. I.; Hamilton, R. J.; Phillips, S. D.; and McCluskey, G. J. Occupational, industrial, and environmental toxicology. 2nded. U.S.A: An Affiliate of Elsevier, Inc., (1997).

[58] Khan, F. I.; and Ghoshal, A. Kr. Removal of volatile organic compounds from polluted air. Journal of Loss Prevention in the Process Industries 13 (2000): 527-545.

[59] Moretti, C. E. Practical solutions for reducing and controlling volatile organic compounds and hazardous air pollutants. New York: American Institute of Chemical Engineers., (2001).

[60] Davis, W. T. Air pollution engineering manual. 2[nd]ed. Canada: John Wiley & Sons, Inc., (1907).

[61] Liu, P. K. T. et al. Engineered bio-filter for removing organic contaminants in air. Journal of Air and Waste Management Association 48 (1994): 299-303.

[62] Ottenger, S. P. P.; and van den Over, A. H. C. Kinetics of organic compound removal from waste gases with a biological filter. Biotechnology and Bioengineering 12 (1983): 3089-3102.

[63] Noyes, R. Handbook of pollution control processes. U.S.A: Noyes Publications., (1991).

[64] Haruta, M. Size – and support-dependency in the catalysis of gold. Catalysis Today 36 (1997): 153-166.

[65] Centeno, M. A.; Paulis, M.; Montes, M.; and Odriozola, J. A. Catalytic combustion of volatile organic compounds on gold/titanium oxynitride catalysts. Applied Catalysis B: Environmental 61 (2005): 177-183.

[66] Kim, K. J.; Kim, Y. H.; and Ahn, H. G. Catalytic performance of nanosized Pt-Au alloy catalyst in oxidation of methanol and toluene. Journal of Nanoscience and Nanotechnology 7 (2007):3795-3799.

[67] Sasahara. T.; Kido, A.; Ishihara. H.; Sunayama. T,; Egashira, M. Highly sensitive detection of volatile organic compounds by an adsorption/combustion-type sensor based on mesoporous silica. Sensors and Actuators B 108 (2005): 478-483.

[68] Qin, H. ; Bao, J. D. ; Hua, T. ; Jin, J. L.; Peng, L.; and Zheng, P. H. Mesoporous silicalite-1 nanospheres and their properties of adsorption and hydrophobicity. Microporous and Mesoporous Materials 129 (2010): 30-36.

[69] Ramos, M. E.; Bonelli, P. R. ; Cukierman, A. L.; Carrott, M. M. L. R. ; and Carrott, P. J. M. Adsorption of volatile organic compounds onto activated carbon cloths derived from a novel regenerated cellulosic precursor. Journal of Hazardous Materials 177 (2010): 175-182.

[70] Kosuge, Katsunori.; Kubo, Shiori.; Kikukawa, Nobuyuki.; and Takemori, Makoto. Effect of pore structure in mesoporous silica on VOC dynamic adsorption /desorption performance. Langmuir 23 (2007): 3095-3102.

[71] Ngeontae, W.; Aeungmaitrepirom, W.; Tuntulani, T.; and Imyim, A. Highly selective preconcentration of Cu(II) from sea water and water samples using amidoamidoxime silica . Talanta 78 (2009): 1004-1010.

[72] Sirikanjanawanit, N. Preparation of gold nanoparticles from jewelry industry wastewater by amido-amidoxime functionalized silica. Master's Thesis, department of chemistry, Faculty of Science, Chulalongkorn University, 2007.

[73] Khanna, P. K.; Gokhale, R.; and Subbarao, V. V. V. S.; et. al. PVA stabilized gold nanoparticles by use of unexplored albeit conventional reducing agent. Materials Chemistry and Physics 92 (2005): 229-233.

APPENDIX

A-1 Adsorption capacity (q) calculation of Au-Ami-SiO$_2$

From standard liquid toluene:

Concentration of standard toluene in methanol	=	$10 \ mg \ L^{-1}$
Injection volume	=	$5 \ \mu L$
Thus, amount of toluene	=	$10 \ \dfrac{mg}{L} \times 5 \ \mu L \times \dfrac{1L}{10^{6} \ \mu L}$
	=	$5 \times 10^{-5} \ mg$
Peak area of standard toluene from GC technique	=	592

From sample toluene vapour :

Injection volume	=	$5 \ \mu L$
For example,　Peak area of non-adsorb toluene	=	6277
Peak area of adsorbed toluene	=	2066
Thus, Peak area from GC technique of adsorbed toluene =		6277 – 2066
	=	4211
Thus, amount of adsorbed toluene	=	$5 \times 10^{-5} mg \times \dfrac{4211}{592}$
	=	$3.56 \times 10^{-4} mg$
At total volume of toluene vapour	=	Flow rate × time
	=	$40 \ \dfrac{mL}{min} \times 15 \min$
	=	$0.6 \ L$
Thus, total amount of toluene	=	$3.56 \times 10^{-4} mg \times \dfrac{0.6L}{5 \mu L} \times \dfrac{10^{6} \ \mu L}{1L}$
	=	$42.7 \ mg$
Adsorbent loading	=	0.05 g
Thus, adsorption capacity (q)	=	$\dfrac{42.7 mg}{0.05 g}$
	=	$854 \ mg \ g^{-1} \ = 0.854 \ g \ g^{-1}$
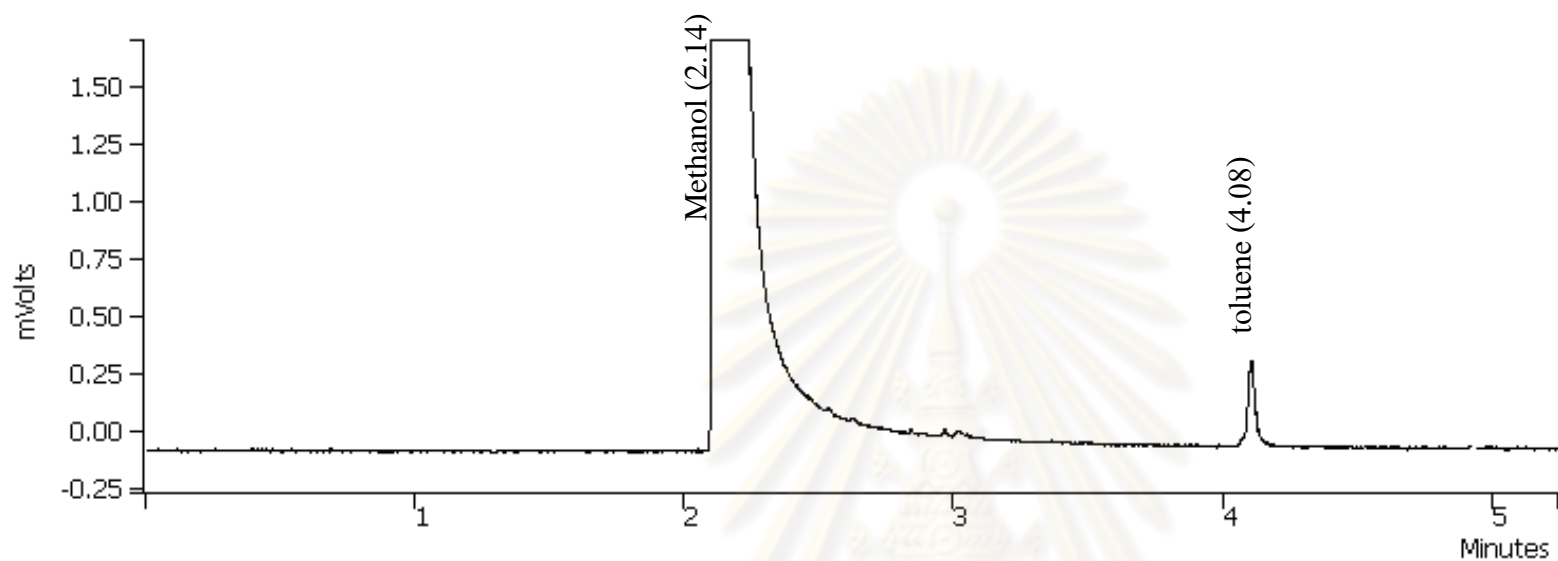
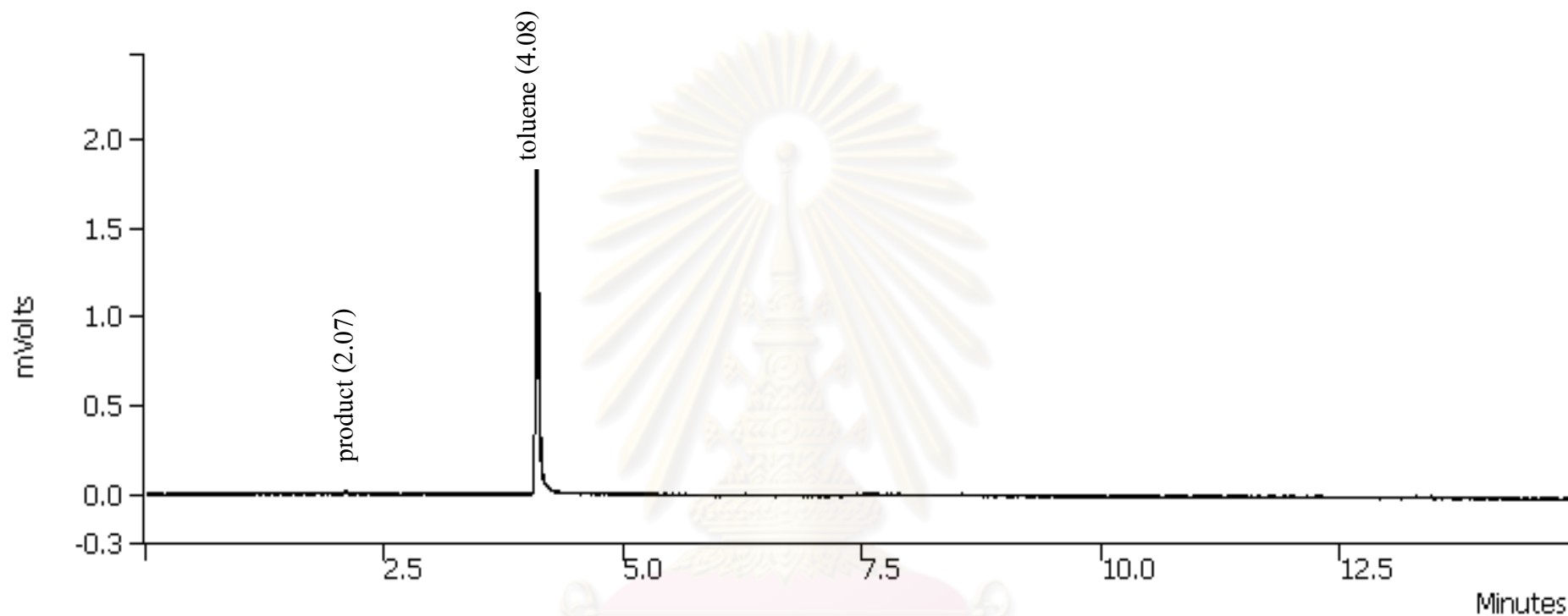**Figure A-2** Gas chromatogram of standard toluene.

Figure A-3 Gas chromatogram of gas product obtained from catalytic oxidation of toluene vapor over Au-Ami-SiO$_2$ catalyst at 175 °C in the continuous system.
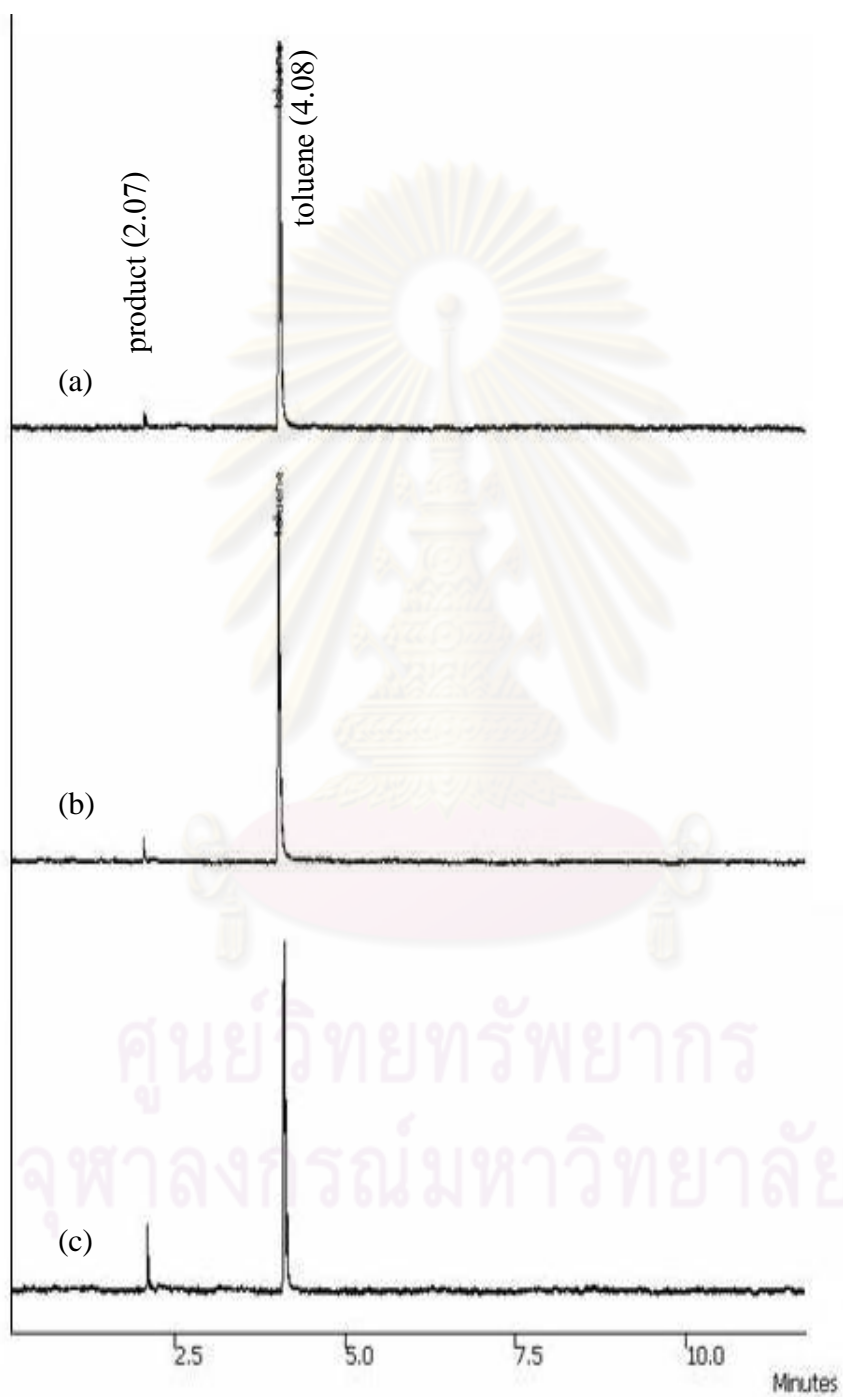
Figure A-4 Gas chromatogram of gas product obtained from catalytic oxidation of toluene vapor over Au-Ami-SiO$_2$ catalyst at (a) 175, (b) 225 and (c) 275 °C in the equilibrium system.
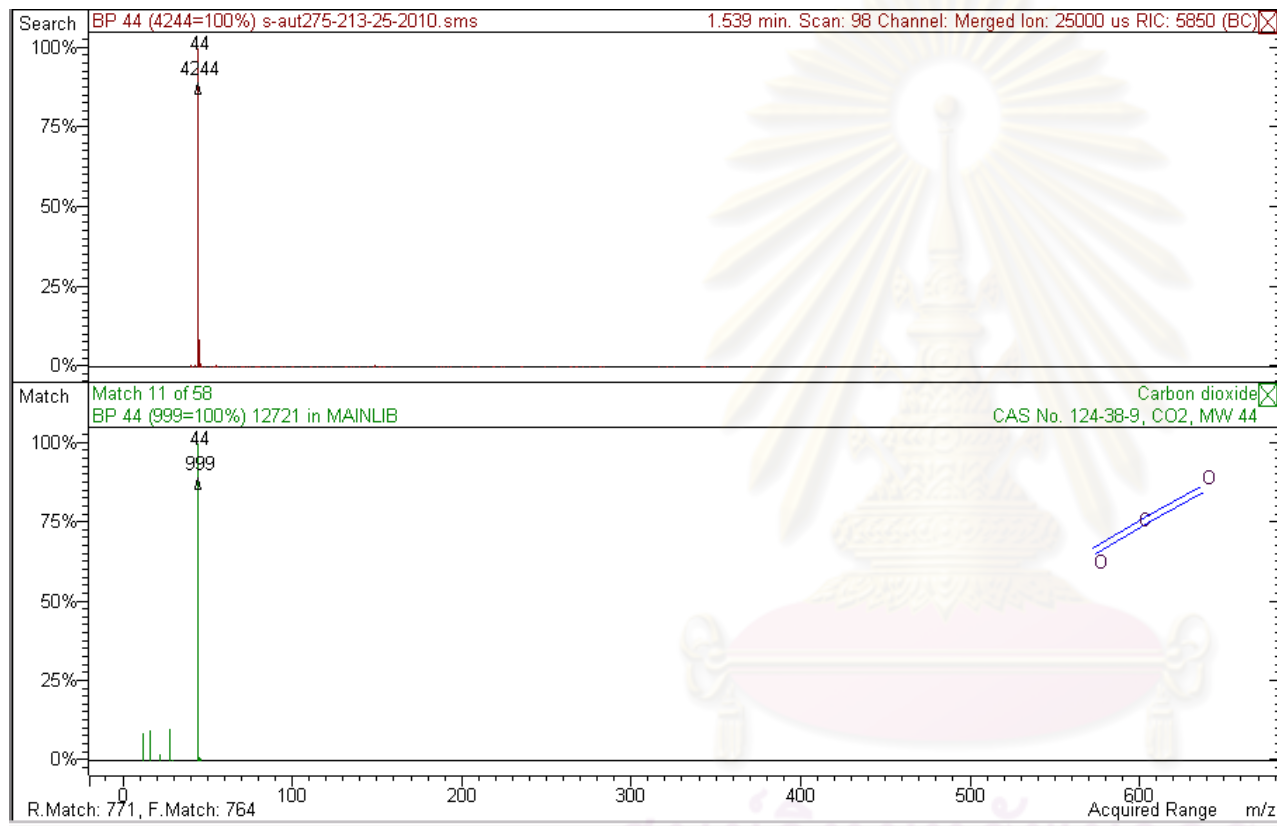
Figure A-5 Mass spectrum of gas product obtained from catalytic oxidation of toluene vapor over Au-Ami-SiO$_2$ catalyst at 275 °C in the equilibrium system.
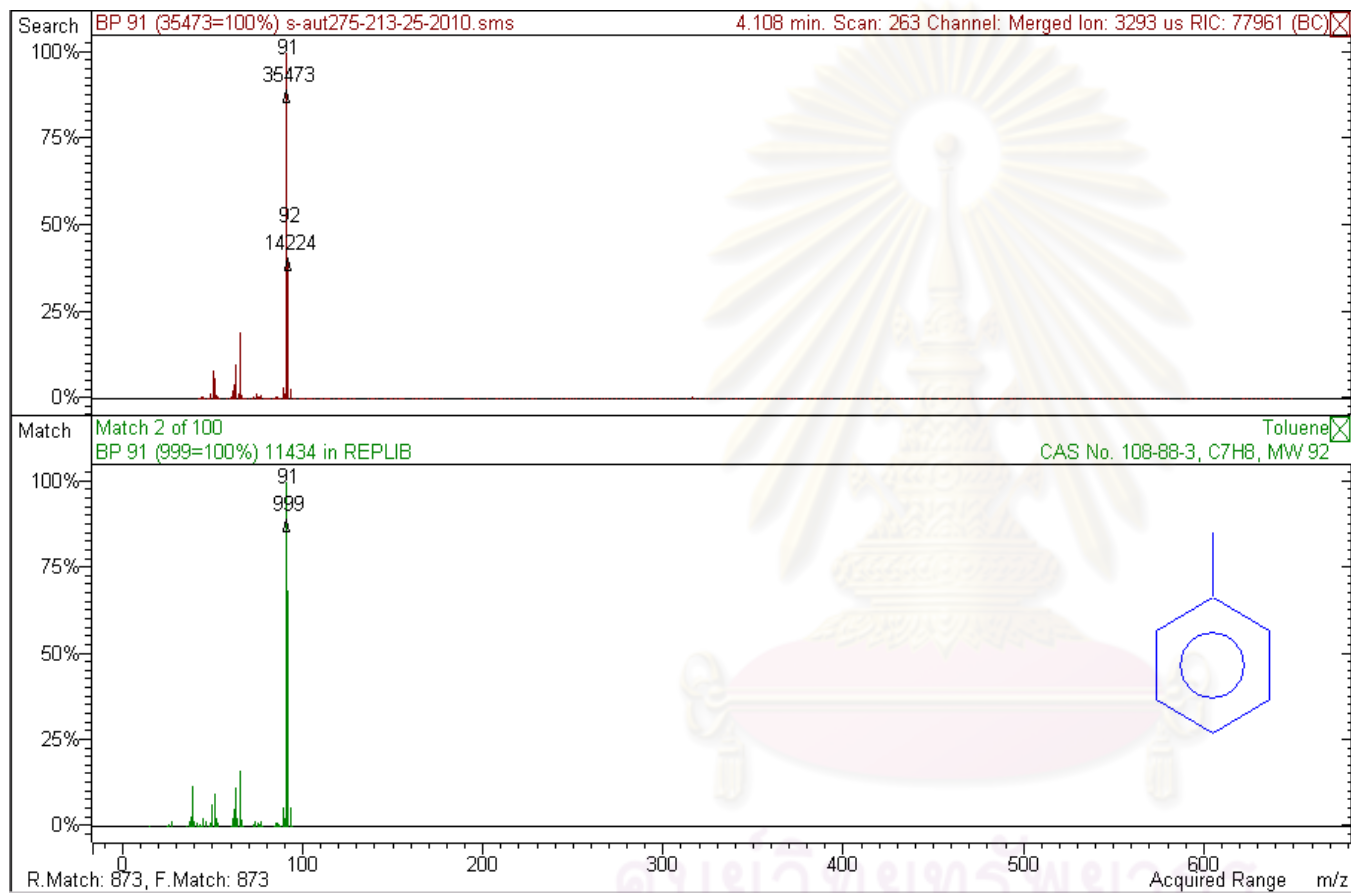
Figure A-5 (continued) Mass spectrum of gas product obtained from catalytic oxidation of toluene vapor over Au-Ami-SiO$_2$ catalyst at 275 °C in the equilibrium system.

VITA

Miss Piyathida Sanghuaypai was born on October 18, 1984 in Nakorn Phanom, Thailand. She received her Bachelor degree of Science in Chemistry from Srinakarinvirot University in 2005. After that, she has been a graduate student at the Program in Petrochemistry and Polymer Science, Faculty of Science, Chulalongkorn University and a member of Environmental Analysis Research Unit. She finished her postgraduate study with the Master degree of Science in 2009. Her present address is 84 Moo 1 Chanaruammit Road, Thauthen, Nakorn Phanom, Thailand, 48120. Contact number is 081-4881146.